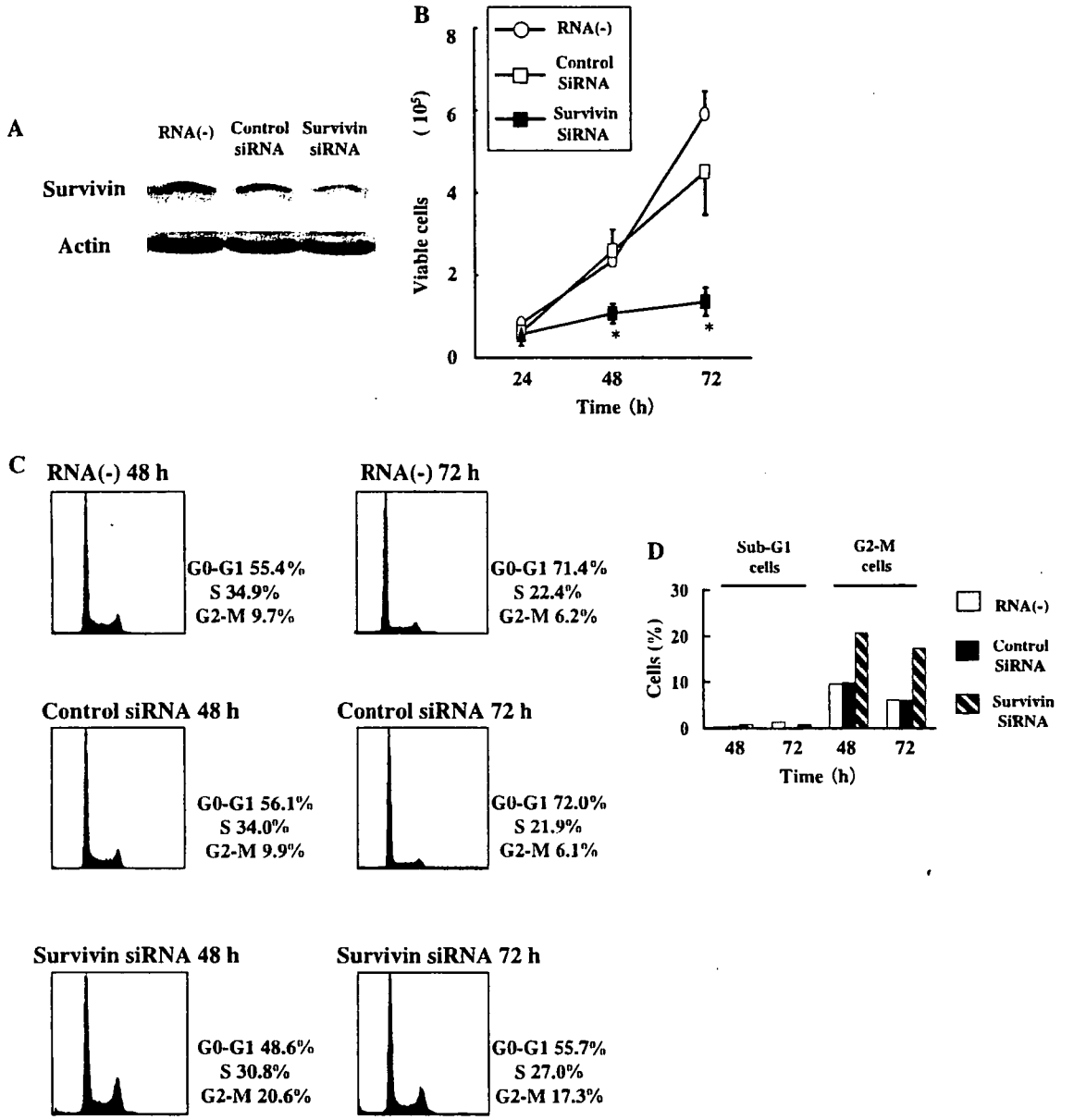

Fig. 4. Effects of survivin depletion by RNAi on the proliferation and cell cycle distribution of A549 cells. (A) Cells were transfected (or not) with a siRNA specific for survivin mRNA or with a control siRNA and were then subjected to immunoblot analysis with antibodies to survivin or to β-actin. Data are representative of three independent experiments. (B) Cells transfected for 24, 48, or 72 h as in (A) were evaluated for cell proliferation by counting the number of viable cells as revealed by staining with trypan blue. Data are means ± SD of values from three independent experiments. $*p < 0.05$ versus the corresponding value for nontransfected cells or cells transfected with the control siRNA. (C) The cell cycle distribution of cells transfected for 48 or 72 h as in (A) was determined by flow cytometry. The percentages of cells at various stages of the cell cycle are indicated. Data are representative of three independent experiments. (D) The percentages of sub-G_1 and G_2–M cells in the experiment shown in (C).

survivin gene by p53 [25]. In contrast, Mirza et al. suggested that chromatin deacetylation in the survivin promoter might contribute to p53-dependent repression of survivin gene expression in the absence of direct binding of p53 to the promoter DNA [26]. In the present study, repression of survivin expression was apparent 24 h after endogenous p53 accumulation, consistent with the results of our previous study [22]. This delay suggests that the mechanism of transcriptional inhibition of the survivin gene by p53 may be indirect. The repression of Cdc2 gene expression by p53 is mediated by a member of the E2F family of transcription factors subsequent to up-regulation of p21 and dephosphorylation of pRB family proteins [17]. However, UV-induced accumulation of p53 and subsequent

down-regulation of survivin have been observed in mouse embryonic fibroblasts derived from p21-null mice [29], suggesting that the ability of p53 to repress survivin gene expression is independent of its ability to up-regulate p21. The molecular mechanism by which p53 induces repression of survivin gene expression in response to DNA damage thus requires further investigation.

To examine the biological consequences of survivin gene repression in cells subjected to DNA damage, we depleted A549 cells of survivin by RNAi. Depletion of survivin resulted in growth arrest in G_2–M phase of the cell cycle, consistent with previous observations [28–31]. Survivin was originally proposed to perform an antiapoptotic function, but this issue remains controversial [29,32]. Indeed, several lines of evidence suggest that survivin plays an important role in regulation of mitotic events [11]. The chromosomal passenger complex (CPC), which consists of Aurora B, INCENP, and survivin, contributes to chromosome segregation and cytokinesis [33]. Depletion or inhibition of survivin or of the other proteins of the CPC thus results in mitotic arrest [30,34]. Furthermore, G_2–M arrest induced by survivin ablation was found to occur in $p53^{+/+}$ cells but not in $p53^{-/-}$ cells, implicating survivin in the p53-dependent G_2–M checkpoint that is essential for maintenance of genomic integrity [29]. Together, these various observations suggest that p53-induced repression of survivin expression in response to DNA damage may lower the threshold for apoptosis in cells in which the p53-dependent G_2–M checkpoint has been activated. Survivin repression following DNA damage may play critical role in deciding if lethal damaged cells die before DNA repair is completed, or if they will have the opportunity to repair and survive. Further characterization of the regulation of survivin in response to DNA damage may provide the basis for potential new approaches to cancer treatment that couple standard cytotoxic DNA-damaging agents with survivin-targeted therapy.

Acknowledgement

We thank Erina Hatashita and Yuki Yamada for technical assistance.

References

[1] G. Ambrosini, C. Adida, D.C. Altieri, A novel anti-apoptosis gene, survivin, expressed in cancer and lymphoma, Nat. Med. 3 (1997) 917–921.

[2] F. Li, D.C. Altieri, Transcriptional analysis of human survivin gene expression, Biochem. J. 344 (1999) 305–311.

[3] F. Li, E.J. Ackermann, C.F. Bennett, A.L. Rothermel, J. Plescia, S. Tognin, A. Villa, P.C. Marchisio, D.C. Altieri, Pleiotropic cell-division defects and apoptosis induced by interference with survivin function, Nat. Cell Biol. 1 (1999) 461–466.

[4] M. Monzo, R. Rosell, E. Felip, J. Astudillo, J.J. Sanchez, J. Maestre, C. Martin, A. Font, A. Barnadas, A. Abad, A novel anti-apoptosis gene: re-expression of survivin messenger RNA as a prognosis marker in non-small-cell lung cancers, J. Clin. Oncol. 17 (1999) 2100–2104.

[5] C. Adida, D. Berrebi, M. Peuchmaur, M. Reyes-Mugica, D.C. Altieri, Anti-apoptosis gene, survivin, and prognosis of neuroblastoma, Lancet 351 (1998) 882–883.

[6] A. Islam, H. Kageyama, N. Takada, T. Kawamoto, H. Takayasu, E. Isogai, M. Ohira, K. Hashizume, H. Kobayashi, Y. Kaneko, A. Nakagawara, High expression of Survivin, mapped to 17q25, is significantly associated with poor prognostic factors and promotes cell survival in human neuroblastoma, Oncogene 19 (2000) 617–623.

[7] H. Kawasaki, D.C. Altieri, C.D. Lu, M. Toyoda, T. Tenjo, N. Tanigawa, Inhibition of apoptosis by survivin predicts shorter survival rates in colorectal cancer, Cancer Res. 58 (1998) 5071–5074.

[8] H. Meng, C.D. Lu, Y.L. Sun, D.J. Dai, S.W. Lee, N. Tanigawa, Expression level of wild-type survivin in gastric cancer is an independent predictor of survival, World J. Gastroenterol. 10 (2004) 3245–3250.

[9] N. Zaffaroni, M.G. Daidone, Survivin expression and resistance to anticancer treatments: perspectives for new therapeutic interventions, Drug Resist. Update 5 (2002) 65–72.

[10] K. Asanuma, R. Moriai, T. Yajima, A. Yagihashi, M. Yamada, D. Kobayashi, N. Watanabe, Survivin as a radioresistance factor in pancreatic cancer, Jpn. J. Cancer Res. 91 (2000) 1204–1209.

[11] R. Honda, R. Korner, E.A. Nigg, Exploring the functional interactions between Aurora B, INCENP, and survivin in mitosis, Mol. Biol. Cell 14 (2003) 3325–3341.

[12] F. Li, G. Ambrosini, E.Y. Chu, J. Plescia, S. Tognin, P.C. Marchisio, D.C. Altieri, Control of apoptosis and mitotic spindle checkpoint by survivin, Nature 396 (1998) 580–584.

[13] R.V. Sionov, Y. Haupt, The cellular response to p53: the decision between life and death, Oncogene 18 (1999) 6145–6157.

[14] B. Vogelstein, D. Lane, A.J. Levine, Surfing the p53 network, Nature 408 (2000) 307–310.

[15] J. Ahn, M. Murphy, S. Kratowicz, A. Wang, A.J. Levine, D.L. George, Down-regulation of the stathmin/Op18 and FKBP25 genes following p53 induction, Oncogene 18 (1999) 5954–5958.

[16] S.A. Innocente, J.L. Abrahamson, J.P. Cogswell, J.M. Lee, p53 regulates a G2 checkpoint through cyclin B1, Proc. Natl. Acad. Sci. USA 96 (1999) 2147–2152.

[17] W.R. Taylor, A.H. Schonthal, J. Galante, G.R. Stark, p130/E2F4 binds to and represses the cdc2 promoter in response to p53, J. Biol. Chem. 276 (2001) 1998–2006.

[18] R. Zhao, K. Gish, M. Murphy, Y. Yin, D. Notterman, W.H. Hoffman, E. Tom, D.H. Mack, A.J. Levine, Analysis of p53-regulated gene expression patterns using oligonucleotide arrays, Genes Dev. 14 (2000) 981–993.

[19] C.D. Lu, D.C. Altieri, N. Tanigawa, Expression of a novel antiapoptosis gene, survivin, correlated with tumor cell apoptosis and p53 accumulation in gastric carcinomas, Cancer Res. 58 (1998) 1808–1812.
[20] A.I. Sarela, C.S. Verbeke, J. Ramsdale, C.L. Davies, A.F. Markham, P.J. Guillou, Expression of survivin, a novel inhibitor of apoptosis and cell cycle regulatory protein, in pancreatic adenocarcinoma, Br. J. Cancer 86 (2002) 886–892.
[21] J. Nakano, C.L. Huang, D. Liu, M. Ueno, S. Sumitomo, H. Yokomise, survivin gene expression is negatively regulated by the p53 tumor suppressor gene in non-small cell lung cancer, Int. J. Oncol. 27 (2005) 1215–1221.
[22] K. Yonesaka, K. Tamura, T. Kurata, T. Satoh, M. Ikeda, M. Fukuoka, K. Nakagawa, Small interfering RNA targeting survivin sensitizes lung cancer cell with mutant p53 to adriamycin, Int. J. Cancer 118 (2005) 812–820.
[23] C. Badie, J.E. Itzhaki, M.J. Sullivan, A.J. Carpenter, A.C. Porter, Repression of CDK1 and other genes with CDE and CHR promoter elements during DNA damage-induced G_2/M arrest in human cells, Mol. Cell. Biol. 20 (2000) 2358–2366.
[24] W.R. Taylor, G.R. Stark, Regulation of the G2/M transition by p53, Oncogene 20 (2001) 1803–1815.
[25] W.H. Hoffman, S. Biade, J.T. Zilfou, J. Chen, M. Murphy, Transcriptional repression of the anti-apoptotic survivin gene by wild type p53, J. Biol. Chem. 277 (2002) 3247–3257.
[26] A. Mirza, M. McGuirk, T.N. Hockenberry, Q. Wu, H. Ashar, S. Black, S.F. Wen, L. Wang, P. Kirschmeier, W.R. Bishop, L.L. Nielsen, C.B. Pickett, S. Liu, Human survivin is negatively regulated by wild-type p53 and participates in p53-dependent apoptotic pathway, Oncogene 21 (2002) 2613–2622.
[27] M. Kappler, H. Taubert, F. Bartel, K. Blumke, M. Panian, H. Schmidt, J. Dunst, M. Bache, Radiosensitization, after a combined treatment of survivin siRNA and irradiation, is correlated with the activation of caspases 3 and 7 in a wt-p53 sarcoma cell line, but not in a mt-p53 sarcoma cell line, Oncol. Rep. 13 (2005) 167–172.
[28] M. Kappler, M. Bache, F. Bartel, M. Kotzsch, M. Panian, P. Wurl, K. Blumke, H. Schmidt, A. Meye, H. Taubert, Knockdown of survivin expression by small interfering RNA reduces the clonogenic survival of human sarcoma cell lines independently of p53, Cancer Gene Ther. 11 (2004) 186–193.
[29] E. Beltrami, J. Plescia, J.C. Wilkinson, C.S. Duckett, D.C. Altieri, Acute ablation of survivin uncovers p53-dependent mitotic checkpoint functions and control of mitochondrial apoptosis, J. Biol. Chem. 279 (2004) 2077–2084.
[30] A. Carvalho, M. Carmena, C. Sambade, W.C. Earnshaw, S.P. Wheatley, Survivin is required for stable checkpoint activation in taxol-treated HeLa cells, J. Cell Sci. 116 (2003) 2987–2998.
[31] S.M. Lens, R.M. Wolthuis, R. Klompmaker, J. Kauw, R. Agami, T. Brummelkamp, G. Kops, R.H. Medema, Survivin is required for a sustained spindle checkpoint arrest in response to lack of tension, EMBO J. 22 (2003) 2934–2947.
[32] J.C. Reed, The Survivin saga goes in vivo, J. Clin. Invest. 108 (2001) 965–969.
[33] M.A. Bolton, W. Lan, S.E. Powers, M.L. McCleland, J. Kuang, P.T. Stukenberg, Aurora B kinase exists in a complex with survivin and INCENP and its kinase activity is stimulated by survivin binding and phosphorylation, Mol. Biol. Cell 13 (2002) 3064–3077.
[34] S. Hauf, R.W. Cole, S. LaTerra, C. Zimmer, G. Schnapp, R. Walter, A. Heckel, J. van Meel, C.L. Rieder, J.M. Peters, The small molecule Hesperadin reveals a role for Aurora B in correcting kinetochore-microtubule attachment and in maintaining the spindle assembly checkpoint, J. Cell Biol. 161 (2003) 281–294.

British Journal of Cancer (2007), 1 – 8

www.bjcancer.com

Full Paper

The novel microtubule-interfering agent TZT-1027 enhances the anticancer effect of radiation *in vitro* and *in vivo*

Y Akashi[1], I Okamoto*[,1], M Suzuki[2], K Tamura[3], T Iwasa[1], S Hisada[4], T Satoh[1], K Nakagawa[1], K Ono[2] and M Fukuoka[1]

[1]Department of Medical Oncology, Kinki University School of Medicine, 377-2 Ohno-higashi, Osaka-Sayama, Osaka 589-8511, Japan; [2]Radiation Oncology Research Laboratory, Research Reactor Institute, Kyoto University, 2-1010 Asashiro-nishi, Kumatori-cho, Sennan-gun, Osaka 590-0494, Japan; [3]Department of Medical Oncology, Kinki University School of Medicine, Nara Hospital, 1248-1 Otodacho, Ikoma,Nara 630-0293, Japan; [4]Asuka Pharmaceutical Co. Ltd, 1604 Shimosakunobe, Takatu-ku, Kawasaki 213-8522, Japan

TZT-1027 is a novel-anticancer agent that inhibits microtubule polymerisation and manifests potent antitumour activity in preclinical models. We have examined the effect of TZT-1027 on cell cycle progression as well as the anticancer activity of this drug both *in vitro* and *in vivo*. With the use of tsFT210 cells, which express a temperature-sensitive mutant of Cdc2, we found that TZT-1027 arrests cell cycle progression in mitosis, the phase of the cell cycle most sensitive to radiation. A clonogenic assay indeed revealed that TZT-1027 increased the sensitivity of H460 cells to γ-radiation, with a dose enhancement factor of 1.2. Furthermore, TZT-1027 increased the radiosensitivity of H460 and A549 cells in nude mice, as revealed by a marked delay in tumour growth and an enhancement factor of 3.0 and 2.2, respectively. TZT-1027 also potentiated the induction of apoptosis in H460 cells by radiation both *in vitro* and *in vivo*. Histological evaluation of H460 tumours revealed that TZT-1027 induced morphological damage to the vascular endothelium followed by extensive central tumour necrosis. Our results thus suggest that TZT-1027 enhances the antitumour effect of ionising radiation, and that this action is attributable in part to potentiation of apoptosis induction and to an antivascular effect. Combined treatment with TZT-1027 and radiation therefore warrants investigation in clinical trials as a potential anticancer strategy.
British Journal of Cancer advance online publication, 1 May 2007; doi:10.1038/sj.bjc.6603769 www.bjcancer.com

Keywords: TZT-1027; radiosensitisation; microtubule; mitotic arrest; apoptosis; antivascular effect

The combination of modalities of cancer treatment offers improvements in the survival of cancer patients compared with individual therapeutic approaches. Such therapeutic benefit has been achieved with combinations of chemo- and radiotherapy in a variety of cancers. The cytotoxicity of most chemotherapeutic agents as well as that of radiation is highly dependent on the phase of the cell cycle. Although various types of anticancer drugs are able to arrest cells at specific cell cycle checkpoints, the ability of antimicrotubule agents to block cell cycle progression in G_2-M phase is the biological basis for combination of these agents with radiation (Pawlik and Keyomarsi, 2004). Microtubule-interfering agents have been shown to increase the radiosensitivity of tumour cells in preclinical and clinical studies (Liebmann *et al*, 1994; Choy *et al*, 1995; Edelstein *et al*, 1996; Vokes *et al*, 1996; Kim *et al*, 2001, 2003; Hofstetter *et al*, 2005; Simoens *et al*, 2006).

TZT-1027 (Soblidotin), a novel microtubule-interfering agent synthesised from dolastatin 10 (Figure 1), exhibits greater antitumour activities and a reduced toxicity compared with its parent compound (Miyazaki *et al*, 1995). TZT-1027 inhibits microtubule assembly by binding to tubulin (Kobayashi *et al*, 1997; Natsume *et al*, 2000). *In vitro*, it inhibits the growth of various human cancer cells at low concentrations (Watanabe *et al*, 2000). *In vivo*, TZT-1027 also manifests a broad spectrum of activity against various murine tumours as well as human tumour xenografts, without inducing a pronounced reduction in body weight (Kobayashi *et al*, 1997; Watanabe *et al*, 2000, 2006a; Natsume *et al*, 2003, 2006). Furthermore, the drug exhibited a potent antivascular effect on existing vasculature in an advanced-stage tumour model (Otani *et al*, 2000). TZT-1027 is currently undergoing clinical evaluation, with a reduction in tumour size and disease stabilisation having been observed in a subset of patients (Schoffski *et al*, 2004; de Jonge *et al*, 2005; Greystoke *et al*, 2006; Tamura *et al*, 2007).

Despite its demonstrated efficacy against solid tumours, the effects of TZT-1027 in combination with radiation have not been examined. As an initial step in determining the antitumour activity of TZT-1027 in combination with radiation, we investigated the effect of this agent on cell cycle progression in synchronised tsFT210 cells (Osada *et al*, 1997), which harbour a temperature-sensitive mutant of Cdc2. We found that TZT-1027 induces arrest of cells in mitosis, the phase of the cell cycle most sensitive to radiation. We then studied the radiosensitising properties of TZT-1027 *in vitro* and *in vivo* with a human lung cancer model and elucidated the mechanism of radiosensitisation by this agent.

*Correspondence: Dr I Okamoto;
E-mail: okamoto@dotd.med.kindai.ac.jp
Revised 28 February 2007; accepted 2 April 2007

MATERIALS AND METHODS

Cell lines and reagents

tsFT210 mouse mammary carcinoma cells, which express a temperature-sensitive mutant of Cdc2, were kindly provided by H Kakeya (Antibiotics Laboratory, Discovery Research Institute, RIKEN, Saitama, Japan) and were maintained under a humidified atmosphere of 5% CO_2 in air at 32.0°C in RPMI 1640 (Sigma, St Louis, MO, USA) supplemented with 10% foetal bovine serum and 1% penicillin-streptomycin. H460 human lung large cell carcinoma and A549 human lung adenocarcinoma cells were obtained from American Type Culture Collection (Manassas, VA, USA) and were maintained as for tsFT210 cells with the exception that the culture temperature was 37°C. TZT-1027 (Figure 1) was provided by Daiichi Pharmaceutical Co. Ltd (Tokyo, Japan). Nocodazole and roscovitine were obtained from Sigma.

Cell cycle analysis

Cells were harvested, washed with phosphate-buffered saline (PBS), fixed with 70% methanol, washed again with PBS, and stained with propidium iodide (0.05 mg ml^{-1}) in a solution containing 0.1% Triton X-100, 0.1 mM EDTA, and RNase A (0.05 mg ml^{-1}). The stained cells ($\sim 1 \times 10^6$) were then analysed for DNA content with a flow cytometer (FACScalibur; Becton Dickinson, San Jose, CA, USA).

Measurement of mitotic index and apoptotic cells

Cells were harvested, washed with PBS, fixed with methanol : acetic acid (3 : 1, v/v), washed again with PBS, and stained with 4′,6-diamidino-2-phenylindole (DAPI) (0.5 μg ml^{-1}). The stained cells ($\sim 1 \times 10^6$) were observed with a fluorescence microscope (IX71; Olympus, Tokyo, Japan). To determine the proportion of mitotic or apoptotic cells, we scored at least 300 cells in each of at least three randomly selected microscopic fields for each of three slides per sample. Cells with condensed chromosomes and no obvious nuclear membrane were regarded as mitotic cells, and the mitotic index was calculated as the percentage of mitotic cells among total viable cells. Cells with fragmented and uniformly condensed nuclei were regarded as apoptotic cells.

Clonogenic assay

Exponentially growing H460 cells in 25-cm^2 flasks were harvested by exposure to trypsin and counted. They were diluted serially to appropriate densities and plated in triplicate in 25-cm^2 flasks containing 10 ml of medium. The cells were treated with 1 nM TZT-1027 or vehicle (dimethyl sulfoxide, or DMSO; final concentration, 0.1%) for 24 h and then exposed to various doses of γ-radiation with a ^{60}Co irradiator at a rate of $\sim$0.82 Gy min^{-1} and at room temperature. The cells were then washed with PBS, cultured in drug-free medium for 10–14 days, fixed with methanol : acetic acid (10 : 1, v/v), and stained with crystal violet. Colonies containing >50 cells were counted. The surviving fraction was calculated as: (mean number of colonies)/(number of inoculated cells × plating efficiency). Plating efficiency was defined as the mean number of colonies divided by the number of inoculated cells for nonirradiated controls. The surviving fraction for combined treatment was corrected by that for TZT-1027 treatment alone. The dose enhancement factor (DEF) was calculated as the dose (Gy) of radiation that yielded a surviving fraction of 0.1 for vehicle-treated cells divided by that for TZT-1027-treated cells (after correction for drug toxicity).

In vivo antitumour activity of TZT-1027 with or without radiation

All animal studies were performed in accordance with the Recommendations for Handling of Laboratory Animals for Biomedical Research, compiled by the Committee on Safety and Ethical Handling Regulations for Laboratory Animal Experiments, Kyoto University. The ethical guidelines followed meet the requirements of the UKCCCR guidelines (Workman *et al*, 1998). Tumour cells (2×10^6) were injected subcutaneously into the right hind leg of 7-week-old female athymic nude mice. Tumour volume was determined from caliper measurement of tumour length (L) and width (W) according to the formula $LW^2/2$. Treatment was initiated when tumours in each group achieved an average volume of $\sim$200–250 mm^3. Treatment groups consisted of control, TZT-1027 alone, radiation alone, and the combination of TZT-1027 and radiation. Each treatment group contained six to eight mice. TZT-1027 was administered intravenously in a single dose of 0.5 mg kg^{-1} of body weight; mice in the control and radiation-alone groups were injected with vehicle (physiological saline). Tumours in the leg were exposed to 10 Gy of γ-radiation with a ^{60}Co irradiator at a rate of $\sim$0.32 Gy min^{-1} immediately after drug treatment. Growth delay (GD) was calculated as the time for treated tumours to achieve an average volume of 500 mm^3 minus the time for control tumours to reach 500 mm^3. The enhancement factor was then determined as: $(GD_{combination} - GD_{TZT-1027})/(GD_{radiation})$.

TUNEL staining

Mice were killed 14 days after treatment initiation and the tumours were removed and preserved in 10% paraformaldehyde. Apoptosis in tumour sections was determined by the terminal deoxynucleotidyl transferase-mediated dUTP-biotin nick-end labelling (TUNEL) assay with the use of an apoptosis detection kit (Chemicon, Temecula, CA, USA). The number of apoptotic cells was counted in 10 separate microscopic fields (× 100) for three sections of each tumour of each group.

Histological analysis

A single dose of TZT-1027 (2.0 mg kg^{-1}) or vehicle (physiological saline) was administered intravenously to mice when H460 tumours had achieved a volume of $\sim$400 to 600 mm^3. Tumour tissue was extirpated 4 or 24 h after drug administration, and half of the tissue was fixed in 10% buffered formalin, embedded in paraffin, sectioned, and stained with hematoxylin-eosin. The other half of the tumour tissue was fixed for 12–48 h in zinc fixative

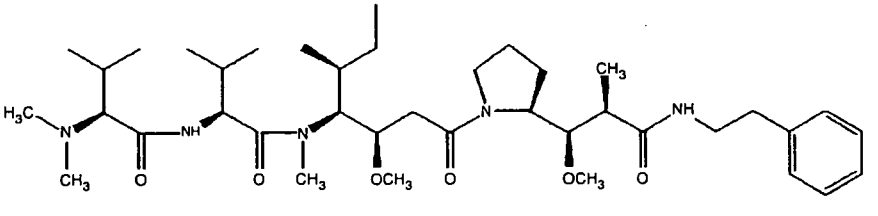

Figure 1 Chemical structure of TZT-1027.

(BD Biosciences, San Jose, CA, USA), embedded in paraffin, sectioned, and immunostained for CD31. Endogenous peroxidase activity was blocked by incubation of the latter sections for 20 min with 0.3% H_2O_2 in methanol, and nonspecific sites were blocked with antibody diluent (Dako Japan, Kyoto, Japan). Sections were then incubated overnight at 4°C with a 1:50 dilution of a rat monoclonal antibody to mouse CD31 (BD Biosciences), washed with PBS, and processed with a Histfine Simple Stain PO (M) kit (Nichirei, Tokyo, Japan) for detection of immune complexes. Sections were counterstained with Mayer's hematoxylin, covered with a coverslip with the use of a permanent mounting medium, and examined with a light microscope (CX41; Olympus, Tokyo, Japan).

Statistical analysis

Data are presented as means ± s.d. or s.e. and were compared by the unpaired Student's *t*-test. A P value of <0.05 was considered statistically significant.

RESULTS

Induction of cell cycle arrest at M phase but not at G_1-S in tsFT210 cells by TZT-1027

To examine the effect of TZT-1027 on cell cycle progression, we performed flow cytometric analysis of tsFT210 cells, which express a temperature-sensitive mutant of Cdc2. These mammary carcinoma cells exhibit a normal cell cycle distribution when incubated at the permissive temperature of 32.0°C, but they arrest at G_2 phase as a result of Cdc2 inactivation when incubated at the nonpermissive temperature of 39.4°C (Figure 2A and B). We synchronised tsFT210 cells at G_2 phase by incubation at 39.4°C for 17 h and then cultured them at 32.0°C for 6 h in the presence of nocodazole (an inhibitor of microtubule polymerisation), TZT-1027, or vehicle (DMSO). In the presence of vehicle alone, the number of cells in G_2 phase decreased markedly and there was a corresponding increase in the number of cells in G_1 phase, indicative of re-entry of cells into the cell cycle (Figure 2C). In contrast, treatment with nocodazole or TZT-1027 prevented the cells from passing through G_2-M phase (Figure 2D and E). Given that flow cytometric analysis did not distinguish between cells in M phase and those in G_2 phase, we determined the mitotic index of cells by DAPI staining and fluorescence microscopy. Most of the cells released from temperature-induced arrest in the presence of nocodazole manifested condensed chromosomes without a nuclear membrane, yielding a mitotic index of 93%; most of the cells had thus arrested in mitosis (Figure 2D). Most of the cells released from temperature-induced arrest in the presence of TZT-1027 showed similar mitotic figures, yielding a mitotic index of 85% (Figure 2E) and demonstrating that TZT-1027 also inhibits cell cycle progression at mitosis.

We next examined whether TZT-1027 affects the G_1-S transition. We arrested tsFT210 cells at G_2 phase by incubation at 39.4°C, released the cells into G_1 phase by shifting to the permissive temperature for 6 h, and then incubated them for an additional 6 h in the presence of roscovitine (an inhibitor of CDK2 that prevents cell cycle progression at G_1 phase), TZT-1027, or vehicle (Figure 3). The cells incubated with vehicle passed through G_1 phase and yielded a broad S-phase peak (Figure 3D), whereas those treated with roscovitine did not pass through G_1 phase (Figure 3E). In contrast, TZT-1027 had no effect on passage of the synchronised tsFT210 cells through the G_1-S transition (Figure 3F). Together,

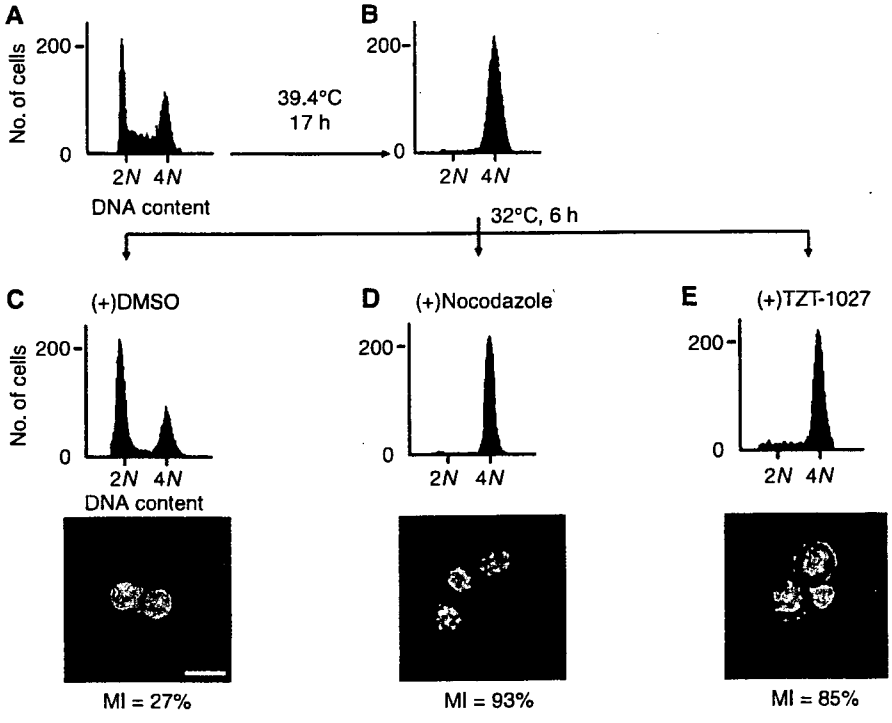

Figure 2 Inhibition of tsFT210 cell cycle progression through G_2-M by TZT-1027. Cells were cultured at the permissive temperature of 32.0°C (**A**) and then incubated for 17 h at the nonpermissive temperature of 39.4°C (**B**). They were subsequently released from G_2 arrest by incubation at 32.0°C for 6 h in the presence of DMSO (**C**), 1 μM nocodazole (**D**), or 2 nM TZT-1027 (**E**). At each stage of the protocol, cells were analysed for DNA content by staining with propidium iodide and flow cytometry. The 2N and 4N peaks indicate cells in G_0-G_1 and G_2-M phases of the cell cycle, respectively. The cells were also stained with DAPI and examined by fluorescence microscopy after treatment with DMSO, nocodazole, or TZT-1027 (lower panels), and the mitotic index (MI) was determined; scale bar, 20 μm. Data are representative of at least three independent experiments.

these results indicate that the effect of TZT-1027 on cell cycle progression is specific to M phase.

Induction of cell cycle arrest at M phase in asynchronous H460 cells by TZT-1027

We next examined whether TZT-1027 induced mitotic arrest in asynchronous H460 human non-small cell lung cancer cells. Flow cytometric analysis revealed that treatment of H460 cells with TZT-1027 for 24 h induced a threefold increase in the proportion of cells with a DNA content of 4N compared with that apparent for vehicle-treated cells (29.1 *vs* 8.7%) (Figure 4A and B). Furthermore, DAPI staining revealed that TZT-1027 induced a significant increase in the mitotic index of H460 cells compared with that for the control cells (23.3 *vs* 4.6%) (Figure 4C and D), indicating that most of the TZT-1027-treated cells with a DNA content of 4N were arrested in M phase rather than in G_2 phase. These observations thus showed that TZT-1027 also induced mitotic arrest in asynchronous H460 cells.

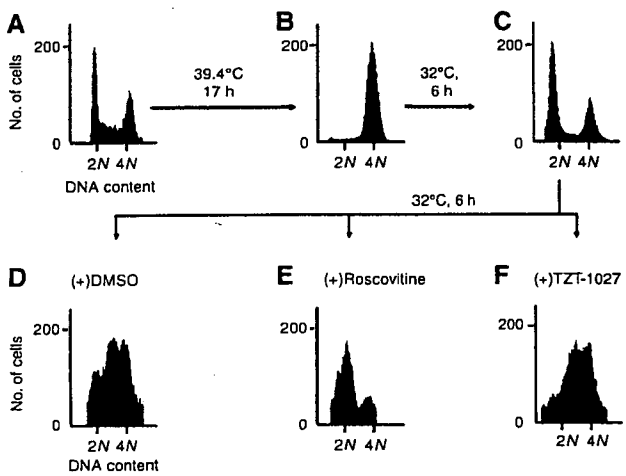

Figure 3 Lack of effect of TZT-1027 on tsFT210 cell cycle progression through G_1-S. Exponentially growing tsFT210 cells (**A**) were arrested in G_2 phase by incubation for 17 h at 39.4°C (**B**). The cells were incubated at 32.0°C first for 6 h to allow progression to G_1 phase (**C**) and then for an additional 6 h in the presence of DMSO (**D**), 50 μM roscovitine (**E**), or 2 nM TZT-1027 (**F**). At each stage of the protocol, cells were analysed for DNA content by flow cytometry. Data are representative of at least three independent experiments.

Radiosensitisation of H460 cells by TZT-1027 *in vitro*

Cells in M phase are more sensitive to radiation than are those in other phases of the cell cycle. Given that exposure of H460 cells to TZT-1027-induced mitotic arrest, we next examined whether this agent might sensitise H460 cells to γ-radiation with the use of a clonogenic assay. H460 cells were incubated for 24 h with 1 nM TZT-1027 or vehicle (DMSO) and then exposed to various doses (0, 2, 4, or 6 Gy) of γ-radiation. The cells were then allowed to form colonies in drug-free medium for 10–14 days. Survival curves revealed that TZT-1027 increased the radiosensitivity of H460 cells, with a DEF of 1.2 (Figure 5A).

To determine whether radiosensitisation by TZT-1027 was reflected by an increase in the proportion of apoptotic cells, we exposed H460 cells to 1 nM TZT-1027 or vehicle for 24 h, treated the cells with various doses (0, 2, 4, or 6 Gy) of radiation, and then incubated them in drug-free medium for an additional 24 h before quantification of apoptosis. Combined treatment with TZT-1027 and 4 or 6 Gy of radiation resulted in a significant increase in the number of apoptotic cells compared with the sum of the values for treatment with drug alone or radiation alone (Figure 5B). TZT-1027 thus promoted radiation-induced apoptosis in H460 cells.

Radiosensitisation of H460 cells and A549 cells by TZT-1027 *in vivo*

To determine whether the TZT-1027-induced increase in the radiosensitivity of tumour cells observed *in vitro* might also be apparent *in vivo*, we injected H460 cells or A549 human lung

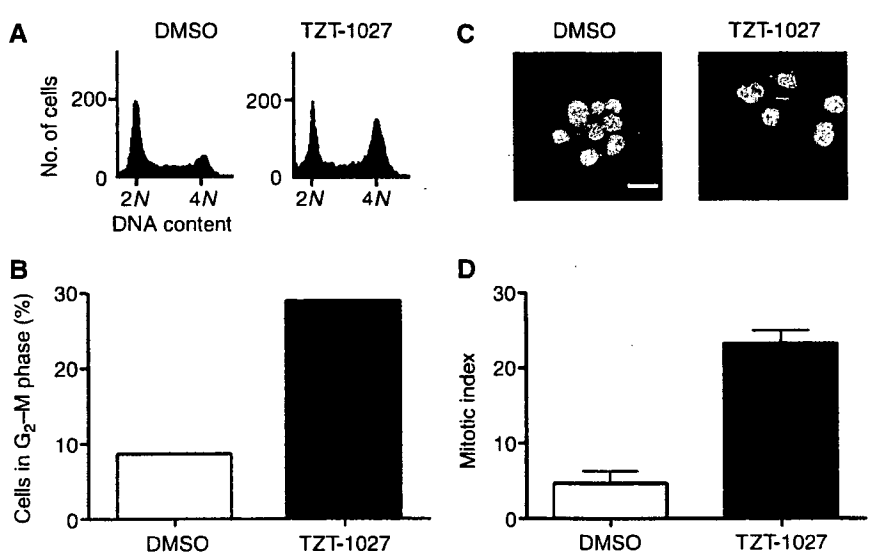

Figure 4 Induction of cell cycle arrest at M phase in H460 cells by TZT-1027. H460 cells were incubated in the presence of 1 nM TZT-1027 or vehicle (DMSO) for 24 h, after which DNA content was measured by flow cytometry (**A**) and the fraction of cells in G_2-M phase was determined (**B**). The cells were also stained with DAPI and examined by fluorescence microscopy (**C**) and the mitotic index was determined (**D**). Data in (**A**) through (**C**) are representative of at least three independent experiments; data in (**D**) are means ± s.d. of values from three independent experiments. Scale bar in (**C**), 20 μm.

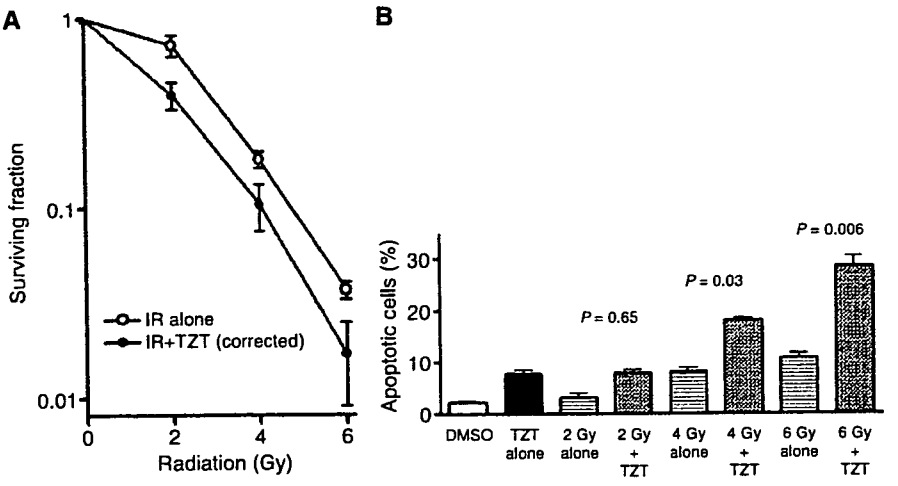

Figure 5 Sensitisation of H460 cells to γ-radiation by TZT-1027 *in vitro*. (**A**) Clonogenic assay. Cells were incubated with 1 nM TZT-1027 or vehicle (DMSO) for 24 h, exposed to the indicated doses of γ-radiation, and then incubated in drug-free medium for 10–14 days for determination of colony-forming ability. Survival curves were generated after correction of colony formation observed for combined treatment with ionising radiation (IR) and TZT-1027 by that apparent for treatment with TZT-1027 alone. (**B**) Assay of apoptosis. Cells were incubated with 1 nM TZT-1027 or vehicle (DMSO) for 24 h, exposed to various doses (0, 2, 4, or 6 Gy) of γ-radiation, and then incubated for 24 h in drug-free medium. Cells were then fixed and stained with DAPI for determination of the proportion of apoptotic cells by fluorescence microscopy. Data in (**A**) and (**B**) are means ± s.d. of values from three independent experiments. *P* values in (**B**) are for comparison of the value for combined treatment with TZT-1027 and radiation *vs* the sum of the corresponding values for each treatment alone, after correction of all data by the control (DMSO) value.

adenocarcinoma cells into nude mice in order to elicit the formation of solid tumours. The mice were then treated with TZT-1027, radiation, or both modalities. Treatment with TZT-1027 alone (single dose of 0.5 mg kg^{-1}) or with radiation alone (single dose of 10 Gy) resulted in relatively small inhibitory effects on tumour growth, whereas combined treatment with both TZT-1027 and radiation exerted a markedly greater inhibitory effect (Figure 6A and B). The tumour GDs induced by treatment with TZT-1027 alone, radiation alone, or both TZT-1027 and radiation were 1.0, 2.6, and 8.8 days, respectively, for H460 cells and 1.4, 4.9, and 12.4 days, respectively, for A549 cells (Table 1). The enhancement factor for the effect of TZT-1027 on the efficacy of radiation was 3.0 for H460 cells and 2.2 for A549 cells, revealing the effect to be greater than additive. No pronounced tissue damage or toxicities such as diarrhoea or weight loss of > 10% were observed in mice in any of the four treatment groups (Table 2).

We examined the effects of the treatment protocols on apoptosis in H460 tumours by TUNEL staining of tumour sections. Quantification of the number of apoptotic cells revealed that the combined treatment with radiation and TZT-1027 induced a significant increase in this parameter compared with treatment with radiation or TZT-1027 alone (Figure 6C).

Histological appearance of H460 tumours after administration of TZT-1027

Finally, we examined whether an effect of TZT-1027 on tumour vasculature might contribute to the antitumour activity of this drug *in vivo*. Mice harbouring H460 tumours were injected with TZT-1027, and the tumours were excised 4 or 24 h thereafter and examined by hematoxylin-eosin staining (Figure 7A–C) or by immunostaining for the endothelial cell marker CD31 (Figure 7D and E). Tumour capillaries appeared congested, with thrombus formation, and showed a loss of endothelial cells 4 h after administration of TZT-1027 (Figure 7B and E), whereas vessels within viable areas of control tumours were generally not congested and showed an intact normal endothelium (Figure 7A and D). The effects of TZT-1027 on the tumour vasculature appeared selective, given that neither loss of CD31 staining nor vessel congestion was apparent in the vasculature of surrounding normal tissue after drug treatment (Figure 7E). Extensive necrosis was apparent at the tumour core, with a characteristic thin rim of viable tumour cells remaining at the periphery, 24 h after TZT-1027 administration (Figure 7C). These results were thus indicative of a characteristic antivascular effect of TZT-1027 in the H460 tumour model.

DISCUSSION

TZT-1027 is a novel antitumour agent that inhibits microtubule polymerisation and exhibits potent antitumour activity in preclinical models (Miyazaki *et al*, 1995; Kobayashi *et al*, 1997; Natsume *et al*, 2000, 2003, 2006; Otani *et al*, 2000; Watanabe *et al*, 2000, 2006a). We investigated the effect of TZT-1027 on cell cycle progression with the use of tsFT210 cells, which can be synchronised in G_2 phase by incubation at 39.4°C and consequent inactivation of Cdc2 (Osada *et al*, 1997; Tamura *et al*, 1999). The use of these cells allows cell synchronisation without the need for agents that prevent DNA synthesis (such as hydroxyurea or thymidine) or that inhibit formation of the mitotic spindle (such as nocodazole). Although such agents halt cell cycle progression in specific phases of the cycle, they are also toxic and kill a proportion of the treated cells. The tsFT210 cell system is thus suited to sensitive analysis of the effects of new compounds on cell cycle progression without loss of cell viability. We have now shown that tsFT210 cells released from G_2 arrest by incubation at 32.0°C failed to pass through M phase in the presence of TZT-1027. Although previous flow cytometric analysis of exponentially growing tumour cells revealed that TZT-1027 induced a marked increase in the proportion of cells in G_2-M (Watanabe *et al*, 2000), it was uncertain whether the drug arrested cell cycle progression in G_2 or in mitosis. Our morphological data now indicate that, similar to the effect of nocodazole, TZT-1027 arrested tsFT210 cells in M phase rather than in G_2, consistent with the mode of action of this new compound. Given that microtubules contribute to various cellular functions in addition to cell division, including intracellular transport and signal transduction (Mollinedo and Gajate,

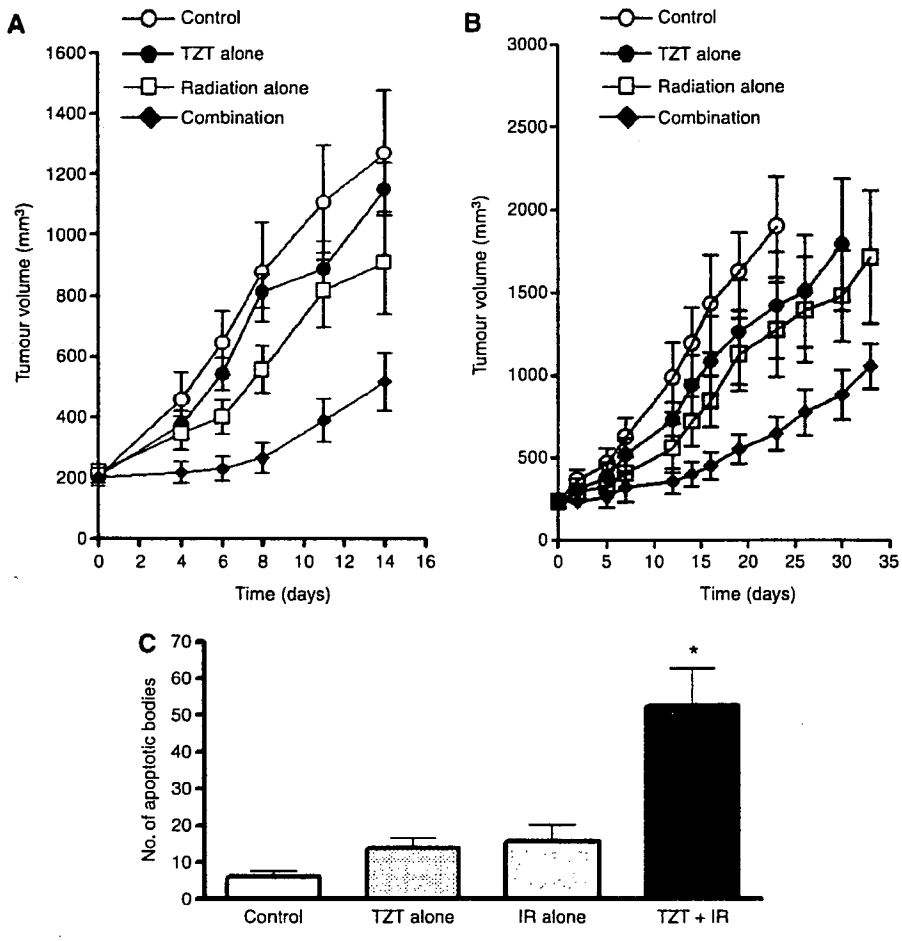

Figure 6 Sensitisation of H460 and A549 cells to γ-radiation by TZT-1027 *in vivo*. (**A** and **B**) Evaluation of tumour growth. Nude mice with H460 (**A**) or A549 (**B**) tumour xenografts (~200 to 250 mm^3) were treated with a single intravenous dose of TZT-1027 (0.5 mg kg^{-1}), a single dose of γ-radiation (10 Gy), or neither (control) or both modalities, and tumour volume was determined at the indicated times thereafter. Data are means ± s.e. for six to eight mice per group. (**C**) Quantification of apoptotic cells in H460 tumour sections by TUNEL staining 14 days after the initiation of treatment as in (**A**). Data are means ± s.d. *$P < 0.05$ *vs* mice treated with TZT-1027 alone or radiation alone.

Table 1 Tumour growth delay value

	H460		A549	
Treatment	**Days[a]**	**GD[b]**	**Days**	**GD**
Control	4.5		5.5	
TZT-1027 alone	5.5	1	6.9	1.4
Radiation alone	7.1	2.6	10.4	4.9
TZT-1027 + Radiation	13.3	8.8	17.9	12.4
Enhancement factor		3		2.2

[a]Days, the period needed for the sizes of xenografts in each group to reach 500 mm^3; [b]GD, the additional periods needed for the sizes of xenografts in each group to reach 500 mm^3 in addition to the period needed for controls to reach 500 mm^3.

Table 2 Body weight loss

	% of B.W.L[a]	
	H460	**A549**
Control	3.6	1.2
TZT-1027 alone	9.9	5.2
Radiation alone	9.7	5.5
TZT-1027+Radiation	8.7	9.9

[a]% of B.W.L, relative body weight loss 7 days after the initiation of the treatment.

2003), TZT-1027 might also be expected to affect tumour cells in interphase. With the use of synchronised tsFT210 cells, however, we found that TZT-1027 had no effect on progression of cells through the G_1–S transition of the cell cycle. The effect of TZT-1027 on cell cycle progression thus appears to be specific to M phase.

Given that cells are most sensitive to radiation during mitosis (Sinclair and Morton, 1966; Sinclair, 1968; Pawlik and Keyomarsi, 2004), we next investigated the possible interaction between TZT-1027 and ionising radiation in human lung cancer cell lines. We found that TZT-1027 increased the sensitivity of H460 cells to γ-radiation *in vitro*. The proportion of H460 cells in mitotic phase at the time of irradiation was increased by TZT-1027 treatment, consistent with the notion that this effect contributes to the observed radiosensitisation induced by this drug. TZT-1027 was previously shown to induce apoptosis in several tumour cell lines (Watanabe *et al*, 2000). Although the relation between apoptosis and radiosensitivity is controversial (Lawrence *et al*, 2001; Pawlik and Keyomarsi, 2004), we showed that treatment of H460 cells with

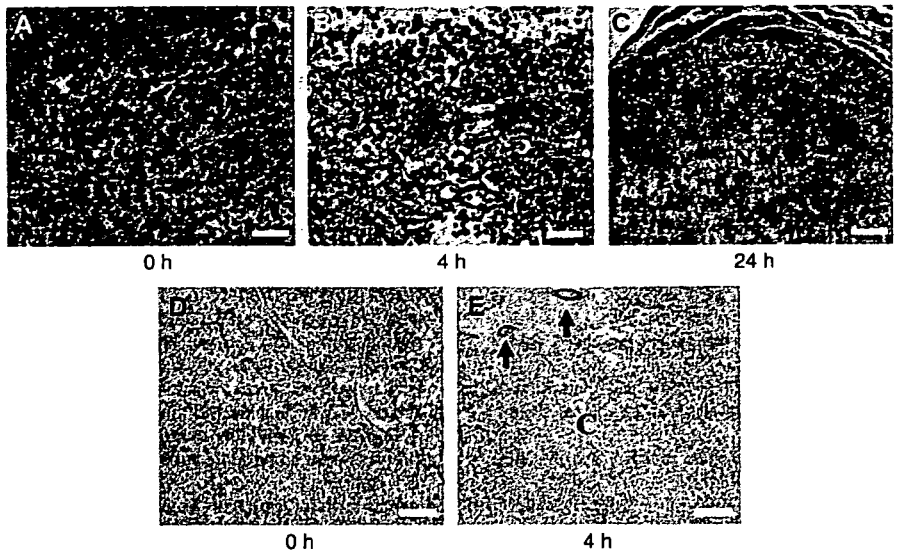

Figure 7 Histological analysis of H460 tumours after treatment with TZT-1027. Mice bearing H460 tumour xenografts were treated with a single dose of TZT-1027 (2.0 mg kg^{-1}), and the tumours were excised at various times thereafter and either stained with hematoxylin-eosin (**A–C**) or immunostained for CD31 (**D** and **E**). (**A** and **D**) Control sections of an untreated tumour showing normal capillaries with an intact endothelium and viable tumour cells. (**B** and **E**) Sections of a tumour removed 4 h after administration of TZT-1027. Vascular congestion, with pink deposits of fibrin, and loss of endothelial cells as well as diffuse tumour cell degeneration are apparent in (**b**). Dark immunostaining of intact endothelium (arrows) is apparent in surrounding normal connective tissue, whereas little staining of endothelial cells was observed in the core (**C**) of the tumour (**E**). (**C**) Section of a tumour removed 24 h after TZT-1027 administration, showing extensive central necrosis (N) and a rim of viable cells (V). Scale bars: 50 μm (**A** and **B**), 100 μm (**C**), and 200 μm (**D** and **E**).

TZT-1027 before irradiation induced a marked increase in the proportion of apoptotic cells compared with that apparent with radiation alone. These results thus suggested that potentiation of apoptosis contributed to radiosensitisation by TZT-1027.

Combined treatment with radiation and a single administration of TZT-1027 also inhibited the growth of tumours formed by H460 or A549 cells *in vivo* to a greater extent than did either treatment alone. Tumour microenvironmental factors, such as the vascular supply, are important determinants of sensitivity to radiation therapy *in vivo*. The ability of microtubule-targeting agents to induce a rapid shutdown of the existing tumour vasculature has been recognised by their designation as vascular-targeting agents (VTAs) (Jordan and Wilson, 2004). Treatment with VTAs such as ZD6126 and combretastatin A-4-P typically results in the destruction of large areas of a tumour, with surviving cells remaining only at the tumour periphery (Dark *et al*, 1997; Blakey *et al*, 2002). These peripheral viable tumour cells presumably derive their nutritional support from nearby normal blood vessels that are not responsive to VTA treatment (Li *et al*, 1998; Siemann and Rojiani, 2002). Such support together with a rapid upregulation of angiogenic factors such as vascular endothelial growth factor may directly facilitate the growth and expansion of the remaining tumour cells (Wachsberger *et al*, 2003; Thorpe, 2004). Given that these residual tumour cells are likely well oxygenated (Wachsberger *et al*, 2003), they are an ideal target for radiation therapy. Several studies have recently shown that treatment with VTAs enhances the therapeutic effect of radiotherapy (Li *et al*, 1998; Siemann and Rojiani, 2002, 2005; Horsman and Murata, 2003; Masunaga *et al*, 2004), consistent with the idea that the components of such combination therapy act in a complementary manner, with VTAs attacking the poorly oxygenated cell population in the central region of tumours and radiation killing the well-oxygenated proliferating cells at the tumour periphery (Li *et al*, 1998; Siemann and Rojiani, 2002; Wachsberger *et al*, 2003). TZT-1027 was previously shown to increase vascular permeability and to induce a decrease in tumour blood flow followed by a marked increase in tissue necrosis in the central region of tumour xenografts (Otani *et al*, 2000; Watanabe *et al*, 2006b). We have now shown that TZT-1027 treatment resulted in congestion and occlusion of tumour blood vessels followed by extensive necrosis of the tumour core, with only a thin rim of viable tumour cells remaining, in the H460 tumour model, suggesting that TZT-1027 acts as a VTA. The action of TZT-1027 as a VTA might thus contribute to the radiosensitising effect observed *in vivo* in the present study.

The clinical use of microtubule-interfering agents such as taxanes in combination with radiation has been successful in improving local tumour control. However, taxanes are often of limited efficacy because of the development of cellular resistance such as that mediated by P-glycoprotein-dependent drug efflux (Goodin *et al*, 2004). The action of TZT-1027 has been suggested to be less affected by multidrug resistance factors, including overexpression of P-glycoprotein, than that of other tubulin inhibitors (Watanabe *et al*, 2006a), suggesting that TZT-1027 may be effective in the treatment of taxane-refractory tumours. Further investigations are thus warranted to examine the combined effects of TZT-1027 and ionising radiation on drug-resistant tumour cells. Whether TZT-1027 enhances the tumour response to clinically relevant fractionated doses of radiation such as 2 Gy per fraction also warrants further study.

In conclusion, we have found that the inhibitory effect of TZT-1027 on cell cycle progression is highly specific to M phase. Moreover, TZT-1027 enhanced the effects of radiation on human cancer cells both *in vitro* and in animal models *in vivo*. These preclinical results provide a rationale for future clinical investigations of the therapeutic efficacy of TZT-1027 in combination with radiotherapy.

ACKNOWLEDGEMENTS

We thank H Kakeya for providing tsFT210 cells as well as M Kobayashi, T Natsume, E Hatashita, Y Yamada, and S Ono for technical assistance.

REFERENCES

Blakey DC, Westwood FR, Walker M, Hughes GD, Davis PD, Ashton SE, Ryan AJ (2002) Antitumor activity of the novel vascular targeting agent ZD6126 in a panel of tumor models. *Clin Cancer Res* **8**: 1974–1983

Choy H, Yee L, Cole BF (1995) Combined-modality therapy for advanced non-small cell lung cancer: paclitaxel and thoracic irradiation. *Semin Oncol* **22**: 38–44

Dark GG, Hill SA, Prise VE, Tozer GM, Pettit GR, Chaplin DJ (1997) Combretastatin A-4, an agent that displays potent and selective toxicity toward tumor vasculature. *Cancer Res* **57**: 1829–1834

de Jonge MJ, van der Gaast A, Planting AS, van Doorn L, Lems A, Boot I, Wanders J, Satomi M, Verweij J (2005) Phase I and pharmacokinetic study of the dolastatin 10 analogue TZT-1027, given on days 1 and 8 of a 3-week cycle in patients with advanced solid tumors. *Clin Cancer Res* **11**: 3806–3813

Edelstein MP, Wolfe III LA, Duch DS (1996) Potentiation of radiation therapy by vinorelbine (Navelbine) in non-small cell lung cancer. *Semin Oncol* **23**: 41–47

Goodin S, Kane MP, Rubin EH (2004) Epothilones: mechanism of action and biologic activity. *J Clin Oncol* **22**: 2015–2025

Greystoke A, Blagden S, Thomas AL, Scott E, Attard G, Molife R, Vidal L, Pacey S, Sarkar D, Jenner A, De-Bono JS, Steward W (2006) A phase I study of intravenous TZT-1027 administered on day 1 and day 8 of a three-weekly cycle in combination with carboplatin given on day 1 alone in patients with advanced solid tumours. *Ann Oncol* **17**: 1313–1319

Hofstetter B, Vuong V, Broggini-Tenzer A, Bodis S, Ciernik IF, Fabbro D, Wartmann M, Folkers G, Pruschy M (2005) Patupilone acts as radiosensitizing agent in multidrug-resistant cancer cells *in vitro* and *in vivo*. *Clin Cancer Res* **11**: 1588–1596

Horsman MR, Murata R (2003) Vascular targeting effects of ZD6126 in a C3H mouse mammary carcinoma and the enhancement of radiation response. *Int J Radiat Oncol Biol Phys* **57**: 1047–1055

Jordan MA, Wilson L (2004) Microtubules as a target for anticancer drugs. *Nat Rev Cancer* **4**: 253–265

Kim JC, Kim JS, Saha D, Cao Q, Shyr Y, Choy H (2003) Potential radiation-sensitizing effect of semisynthetic epothilone B in human lung cancer cells. *Radiother Oncol* **68**: 305–313

Kim JS, Amorino GP, Pyo H, Cao Q, Price JO, Choy H (2001) The novel taxane analogs, BMS-184476 and BMS-188797, potentiate the effects of radiation therapy *in vitro* and *in vivo* against human lung cancer cells. *Int J Radiat Oncol Biol Phys* **51**: 525–534

Kobayashi M, Natsume T, Tamaoki S, Watanabe J, Asano H, Mikami T, Miyasaka K, Miyazaki K, Gondo M, Sakakibara K, Tsukagoshi S (1997) Antitumor activity of TZT-1027, a novel dolastatin 10 derivative. *Jpn J Cancer Res* **88**: 316–327

Lawrence TS, Davis MA, Hough A, Rehemtulla A (2001) The role of apoptosis in 2′,2′-difluoro-2′-deoxycytidine (gemcitabine)-mediated radiosensitization. *Clin Cancer Res* **7**: 314–319

Li L, Rojiani A, Siemann DW (1998) Targeting the tumor vasculature with combretastatin A-4 disodium phosphate: effects on radiation therapy. *Int J Radiat Oncol Biol Phys* **42**: 899–903

Liebmann J, Cook JA, Fisher J, Teague D, Mitchell JB (1994) *In vitro* studies of Taxol as a radiation sensitizer in human tumor cells. *J Natl Cancer Inst* **86**: 441–446

Masunaga S, Sakurai Y, Suzuki M, Nagata K, Maruhashi A, Kinash Y, Ono K (2004) Combination of the vascular targeting agent ZD6126 with boron neutron capture therapy. *Int J Radiat Oncol Biol Phys* **60**: 920–927

Miyazaki K, Kobayashi M, Natsume T, Gondo M, Mikami T, Sakakibara K, Tsukagoshi S (1995) Synthesis and antitumor activity of novel dolastatin 10 analogs. *Chem Pharm Bull (Tokyo)* **43**: 1706–1718

Mollinedo F, Gajate C (2003) Microtubules, microtubule-interfering agents and apoptosis. *Apoptosis* **8**: 413–450

Natsume T, Watanabe J, Horiuchi T, Kobayashi M (2006) Combination effect of TZT-1027 (Soblidotin) with other anticancer drugs. *Anticancer Res* **26**: 1145–1151

Natsume T, Watanabe J, Koh Y, Fujio N, Ohe Y, Horiuchi T, Saijo N, Nishio K, Kobayashi M (2003) Antitumor activity of TZT-1027 (Soblidotin) against vascular endothelial growth factor-secreting human lung cancer *in vivo*. *Cancer Sci* **94**: 826–833

Natsume T, Watanabe J, Tamaoki S, Fujio N, Miyasaka K, Kobayashi M (2000) Characterization of the interaction of TZT-1027, a potent antitumor agent, with tubulin. *Jpn J Cancer Res* **91**: 737–747

Osada H, Cui CB, Onose R, Hanaoka F (1997) Screening of cell cycle inhibitors from microbial metabolites by a bioassay using a mouse cdc2 mutant cell line, tsFT210. *Bioorg Med Chem* **5**: 193–203

Otani M, Natsume T, Watanabe JI, Kobayashi M, Murakoshi M, Mikami T, Nakayama T (2000) TZT-1027, an antimicrotubule agent, attacks tumor vasculature and induces tumor cell death. *Jpn J Cancer Res* **91**: 837–844

Pawlik TM, Keyomarsi K (2004) Role of cell cycle in mediating sensitivity to radiotherapy. *Int J Radiat Oncol Biol Phys* **59**: 928–942

Schoffski P, Thate B, Beutel G, Bolte O, Otto D, Hofmann M, Ganser A, Jenner A, Cheverton P, Wanders J, Oguma T, Atsumi R, Satomi M (2004) Phase I and pharmacokinetic study of TZT-1027, a novel synthetic dolastatin 10 derivative, administered as a 1-hour intravenous infusion every 3 weeks in patients with advanced refractory cancer. *Ann Oncol* **15**: 671–679

Siemann DW, Rojiani AM (2002) Enhancement of radiation therapy by the novel vascular targeting agent ZD6126. *Int J Radiat Oncol Biol Phys* **53**: 164–171

Siemann DW, Rojiani AM (2005) The vascular disrupting agent ZD6126 shows increased antitumor efficacy and enhanced radiation response in large, advanced tumors. *Int J Radiat Oncol Biol Phys* **62**: 846–853

Simoens C, Vermorken JB, Korst AE, Pauwels B, De Pooter CM, Pattyn GG, Lambrechts HA, Breillout F, Lardon F (2006) Cell cycle effects of vinflunine, the most recent promising Vinca alkaloid, and its interaction with radiation, *in vitro*. *Cancer Chemother Pharmacol* **58**: 210–218

Sinclair WK (1968) Cyclic x-ray responses in mammalian cells *in vitro*. *Radiat Res* **33**: 620–643

Sinclair WK, Morton RA (1966) X-ray sensitivity during the cell generation cycle of cultured Chinese hamster cells. *Radiat Res* **29**: 450–474

Tamura K, Nakagawa K, Kurata T, Satoh T, Nogami T, Takeda K, Mitsuoka S, Yoshimura N, Kudoh S, Negoro S, Fukuoka M (2007) Phase I study of TZT-1027, a novel synthetic dolastatin 10 derivative and inhibitor of tubulin polymerization, which was administered to patients with advanced solid tumors on days 1 and 8 in 3-week courses. *Cancer Chemother Pharmacol* (in press)

Tamura K, Rice RL, Wipf P, Lazo JS (1999) Dual G_1 and G_2/M phase inhibition by SC-alpha alpha delta 9, a combinatorially derived Cdc25 phosphatase inhibitor. *Oncogene* **18**: 6989–6996

Thorpe PE (2004) Vascular targeting agents as cancer therapeutics. *Clin Cancer Res* **10**: 415–427

Vokes EE, Haraf DJ, Masters GA, Hoffman PC, Drinkard LC, Ferguson M, Olak J, Watson S, Golomb HM (1996) Vinorelbine (Navelbine), cisplatin, and concomitant radiation therapy for advanced malignancies of the chest: a Phase I study. *Semin Oncol* **23**: 48–52

Wachsberger P, Burd R, Dicker AP (2003) Tumor response to ionizing radiation combined with antiangiogenesis or vascular targeting agents: exploring mechanisms of interaction. *Clin Cancer Res* **9**: 1957–1971

Watanabe J, Minami M, Kobayashi M, Natsume T, Watanabe J, Horiuchi T, Kobayashi M (2006a) Antitumor activity of TZT-1027 (Soblidotin). *Anticancer Res* **26**: 1973–1981

Watanabe J, Natsume T, Fujio N, Miyasaka K, Kobayashi M (2000) Induction of apoptosis in human cancer cells by TZT-1027, an antimicrotubule agent. *Apoptosis* **5**: 345–353

Watanabe J, Natsume T, Kobayashi M (2006b) Antivascular effects of TZT-1027 (Soblidotin) on murine Colon26 adenocarcinoma. *Cancer Sci* **97**: 1410–1416

Workman P, Twentyman P, Balkwill F, Balmain A, Chaplin D, Double J, Embleton J, Newell D, Raymond R, Stables J, Stephens T, Wallace J (1998) United Kingdom Co-ordinating Committee on Cancer Research (UKCCCR) Guidelines for the Welfare of Animals in Experimental Neoplasia 2nd edn. *Br J Cancer* **77**: 1–10

Int J Clin Oncol (2007) 12:218–223
DOI 10.1007/s10147-007-0658-x

ORIGINAL ARTICLE

Toshio Shimizu · Taroh Satoh · Kenji Tamura
Tomohiro Ozaki · Isamu Okamoto · Masahiro Fukuoka
Kazuhiko Nakagawa

Oxaliplatin/fluorouracil/leucovorin (FOLFOX4 and modified FOLFOX6) in patients with refractory or advanced colorectal cancer: post-approval Japanese population experience

Received: August 16, 2006 / Accepted: January 10, 2007

Abstract
Background. The oxaliplatin/fluorouracil/leucovorin (FOLFOX regimen) is an effective and generally well-tolerated regimen in Western clinical studies of advanced colorectal cancer. In Japan, oxaliplatin was approved in April 2005.
Methods. To evaluate the objective tumor responses and feasibility (toxicities) of FOLFOX regimens (FOLFOX4 and modified FOLFOX6, mFOLFOX6) in a predominantly Japanese population with refractory or advanced colorectal cancer in Japan, 51 consecutive patients with histologically confirmed metastatic colon or rectum cancer who were treated between April 2005 and March 2006 were enrolled in a retrospective study. FOLFOX4 was used for treatment in 39% (first-line, 45%) of these patients, and mFOLFOX6 was used for treatment in 61% (first-line, 61%). Tumor responses were assessed radiologically, and toxicities were graded according to the Common Terminology Criteria for Adverse Events (CTCAE) version 3.0 regarding toxicities other than peripheral sensory neuropathy.
Results. The objective response rates (in those who underwent first- or second-line therapy) were 50.0% and 8.7%, respectively. The tumor control rate (partial response [PR] + stable disease [SD]) was 80.4%. There were no toxicity-related deaths. Neutropenia grade 3 was experienced in 20% of patients, and often caused delay in the subsequent treatment course. Mild to moderate cumulative peripheral sensory neuropathy affected 78% of patients. The incidence of hypersensitivity reactions to oxaliplatin in our study was lower than that in reported in Western countries.
Conclusion. Both FOLFOX regimens have good efficacy in refractory or advanced colorectal cancer in a Japanese population, with an acceptable overall toxicity profile.

T. Shimizu (✉) · K. Tamura · T. Ozaki
Department of Medical Oncology, Kinki University Nara Hospital, 1248-1 Otoda-cho, Ikoma, Nara 630-0293, Japan
Tel. +81-743-77-0880; Fax +81-743-77-0890
e-mail: tshimizu@nara.med.kindai.ac.jp

T. Satoh · I. Okamoto · M. Fukuoka · K. Nakagawa
Department of Medical Oncology, Kinki University School of Medicine, Osaka, Japan

Key words Oxaliplatin · FOLFOX · Colorectal cancer · Japanese population

Introduction

In 2000, it has reported that colorectal cancer (CRC) was diagnosed in more than 90000 patients per year in Japan, resulting in 36000 deaths per year.

Colorectal cancer accounts for 10% to 15% of all cancers and is the third leading cause of cancer-related death in Western countries. Approximately one-half of all patients develop metastatic disease. The prognosis for these patients is poor, although palliative chemotherapy has been shown to be able to prolong survival and improve the quality of life over best supportive care. For many years, the treatment of metastatic colorectal cancer was restricted to 5-fluorouracil (5FU) and the biomodulation of this agent.[1] Oxaliplatin and irinotecan, combined with continuous infusion of 5FU, significantly improved response rate, progression-free survival (PFS), and overall survival.[2–4] FOLFOX4 (oxaliplatin and leucovorin [LV] 5FU2) is more active than LV5FU2 alone, and has also shown superiority over IFL (irinotecan, FU bolus, leucovorin). Oxaliplatin (L-OHP), a new third-generation 1,2-DACH-platinum derivative, has a mechanism of action similar to that of other platinum derivatives.[5–9] However, its spectrum of antitumor activity in tumor models differs from those of cisplatin and carboplatin. In addition, it has also been observed to demonstrate activity against cisplatin-resistant colon carcinoma cell lines.[10] In addition, experimental data have shown synergistic activity of the oxaliplatin/FU combination. The clinical toxicity of oxaliplatin is also distinct from that of other platinum drugs: it has no renal toxicity and minimal hematotoxicity; it causes both a reversible acute, cold-related dysesthesia and a dose-limiting cumulative peripheral sensory neuropathy that usually regresses rapidly after treatment withdrawal. The recent availability of five active chemotherapeutic agents has doubled the median overall survival for metastatic CRC from 10 to 20 months.

Three combinations have shown excellent first-line efficacy in phase III trials – IFL with bevacizumab, FOLFOX, and FOLFIRI – however, neither of these combinations is clearly superior. Our clinical practice in Japan has been guided in a major way by extrapolation from the results of clinical trials conducted mainly in Western countries. To evaluate the value of FOLFOX regimens in the treatment of refractory or advanced CRC, a retrospective analysis study was designed to assess the feasibility (toxicities) and efficacy of combining oxaliplatin with the LV5FU2 schedule in a Japanese population. We herein report our experience with two FOLFOX regimens (FOLFOX4 and modified [m] FOLFOX6) in patients with advanced CRC, specifically, the toxicities and objective tumor response rates obtained.

Patients and methods

A retrospective analysis study was conducted at Kinki University Hospital in 51 consecutive patients with histologically confirmed metastatic colon or rectum cancer who were treated between April 2005 and March 2006. The primary objectives were to assess the feasibility (toxicities) and efficacy of two FOLFOX regimens (FOLFOX4 and mFOLFOX6) in a Japanese population. FOLFOX4 is a regimen comprising oxaliplatin 85 mg/m^2 as a 2-h infusion (day 1); LV 100/m^2 per day as a 2-h infusion (days 1 and 2); followed by a 5FU bolus 400 mg/m^2 per day and 5FU 600 mg/m^2 per day as a 22-h infusion (days 1 and 2). mFOLFOX6 is a regimen also comprising oxaliplatin 85 mg/m^2 as a 2-h infusion (day 1), LV 200 mg/m^{2}per day as a 2-h infusion (day 1), followed by a 5FU bolus 400 mg/m^2 (day 1) and 5FU 2400 mg/m^2 per day as a 46-h infusion (days 1 to 2). These therapies were administered on day 1 and repeated on day 2 of a 14-day treatment cycle. Routine antiemetic prophylaxis with a serotonin (5-HT3) antagonist (granisetron) and dexamethasone was given (Fig. 1). The use of implantable ports and infusion pumps allowed chemotherapy to be administered on an outpatient basis in some cases. Treatment was continued until either disease progression, the occurrence of unacceptable toxicity, or the patient refused further treatment. Toxicity was graded according to the Common Terminology Criteria for Adverse Events (CTCAE) version 3.0 regarding toxicities other than peripheral sensory neuropathy and by following the oxaliplatin-specific scale (DEB-NTC). The definitions in the oxaliplatin-specific scale, which was developed as a specific scoring scale for oxaliplatin-inducing peripheral sensory neuropathy, are as follows: grade 1, transient dysesthesia and/or paresthesia lasting for less than 7 days; grade 2, transient dysesthesia and/or paresthesia lasting for 7 days or longer; and grade 3, dysesthesia and/or paresthesia with pain or function impairment that interferes with activities of daily living (such as difficulty with fastening buttons and writing). The response of measurable target lesions to treatment was objectively evaluated according to the Response Evaluation Criteria in Solid Tumors (RECIST) criteria after each four cycles of treatment. Complete response (CR) was defined as the disappearance of all disease. Partial response (PR) was defined as at least a 30% reduction in the sum of the longest diameters of all measured lesions by at least 4 weeks. Progressive disease (PD) was defined as an increase in lesions by 20%

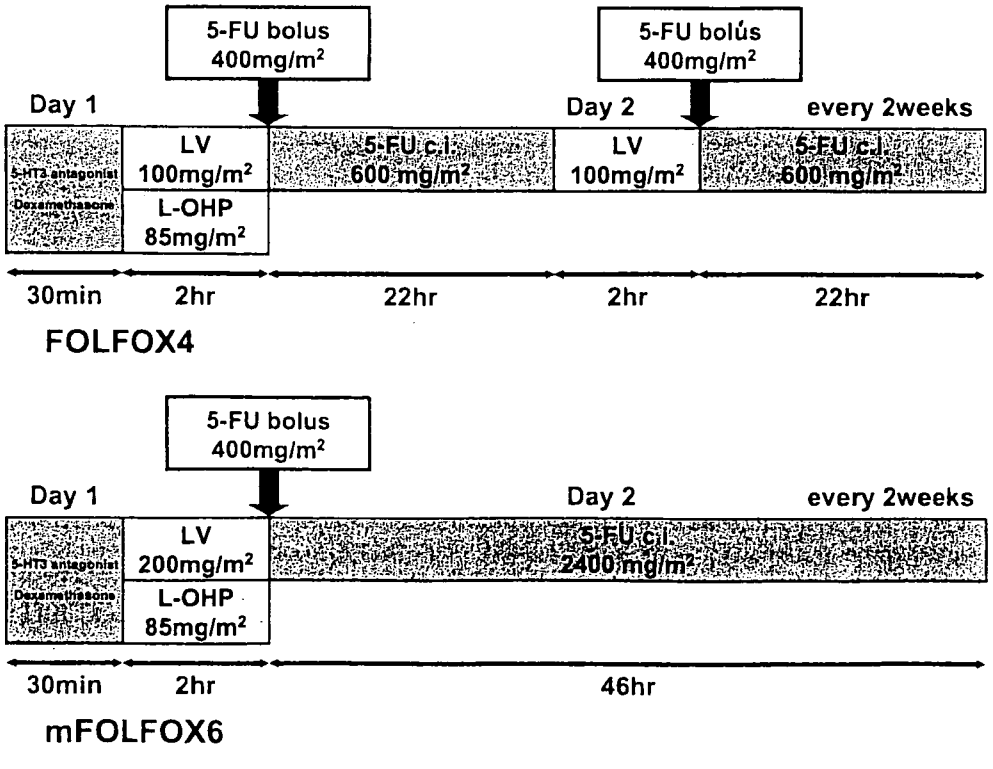

Fig. 1. Treatment schema for FOLFOX4 and mFOLFOX6 regimens. *LV*, leucovorin; *5-FU*, 5-fluorouracil; *L-OHP*, oxaliplatin; *c.i.*, continuous infusion

or greater, or the appearance of new lesions. Responses not falling into any of these categories were classified as stable disease (SD).

Results

Patient characteristics

A total of 51 patients with a median age of 61 years (range, 34–78 years) with refractory or advanced CRC were retrospectively analyzed. The patients' characteristics are listed in Table 1. Patients were treated with the FOLFOX4 (39%) or mFOLFOX6 regimens (61%). Twenty-eight patients (55%; FOLFOX4, 9; mFOLFOX6, 19) were treated in a first-line setting, and 23 patients (45%; FOLFOX4, 11; mFOLFOX6, 12) were treated in a second-line setting. Since April 2005, 4 months prior to beginning this study, we have used the FOLFOX4 regimen for inpatients, and from that time we selected the mFOLFOX6 regimen for all patients in the outpatient setting. The total number of chemotherapy cycles administered was 384, with a median of 8 cycles per patient (range, 1–12 cycles). The median dose intensity (actual/planned dose) was 93.4% for oxaliplatin and 100% for 5FU in the FOLFOX4 group and 91.2% for oxaliplatin and 94.8% for 5FU in the mFOLFOX6 group. The median dose intensity of oxaliplatin was 37 mg/m^2 per week (range, 31–42 mg/m^2 per week) in the FOLFOX4 group and 34 mg/m^2 per week (range, 23–42 mg/m^2 per week) in the mFOLFOX6 group.

Hematological toxicity

Several pertinent hematological toxicities are listed in Table 2, shown with numbers of patients who experienced them. The onset of neutropenia typically occurred between 10 and 14 days after treatment. Grade 3 and 4 neutropenia was observed in 20% of patients, with neutropenic fever being uncommon. Neutropenia often caused delay in the start of a subsequent treatment course. In all, 88 (23%) of 384 cycles were delayed due to toxicity, most commonly hematological: 64 (17%) for neutropenia and 24 (6%) for neurotoxicity. Using our administration schedule, no thrombocytopenia of over grade 3 was observed to develop. In addition, only one patient developed grade 3 anemia with transfusion.

Nonhematological toxicity

The most common nonhematological adverse effects of the FOLFOX regimens were peripheral neuropathy and lethargy (fatigue). These effects are listed in Table 3. Two patients experienced grade 2 hypersensitivity reactions (rash/hives, erythema, and one patient also experienced vomiting) during the administration of oxaliplatin. The symptoms rapidly resolved, in a few minutes, on symptomatic treatment (termination of infusion, use of steroids, and antagonists of type 1 and 2 histamine receptors). In using successful strategies over the next treatment courses (slowing the infusion rate, increasing the doses of steroids, and dose reduction of oxaliplatin), both patients were able to tolerate rechallenge of oxaliplatin, and one patient achieved a partial response. Peripheral neurotoxicity, characterized by paresthesia in a symmetric, glove-and-stocking distribution, occurred in 40 (78%) patients and there was no grade over 3.

Whenever the number of treatment cycles increases, neuropathy, within grade 2 level, tends to increase. The incidence of neurotoxicity along with the number of treatment cycles is listed in Table 4. Cold-related dysesthesia

Table 1. Characteristics of the study patients

Characteristics	$n = 51$
Sex, male/female	28/23
Age, years, median (range)	61 (34–78)
Performance status (ECOG), 0/1/2	19/25/7
Primary tumor, colon/rectum/rectosigmoid	28/20/3
Adjuvant therapy, +/–	18/33
Previous irinotecan therapy, +/–	15/36
Site of metastases, lung/liver/LN/peritoneum	22/21/18/7
FOLFOX4/mFOLFOX6	20/31
First-line/second-line	28/23
Dose reduction: +/–	7/44

ECOG, Eastern Cooperative Oncology Group; LN, distant lymph nodes

Table 2. Hematological toxicity (CTCAE V3.0)

	$n = 51$					
	Grade 1	Grade 2	Grade 3	Grade 4	All grades	Grade ≧3
Leucocytopenia	17	16	1	0	67%	2%
Neutropenia	18	15	9	1	84%	20%
Anemia	19	8	1	0	55%	2%
Thrombocytopenia	23	5	0	0	55%	0%

Table 3. Nonhematological toxicity (CTCAE V3.0)*

	$n = 51$					
	Grade 1	Grade 2	Grade 3	Grade 4	All grades	Grade ≧3
Anorexia	16	2	2	0	39%	4%
Nausea	13	2	2	0	33%	4%
Vomiting	5	2	2	0	18%	4%
Mucositis	10	1	2	0	25%	4%
Febrile neutropenia	–	–	0	0	0%	–
Hand-foot syndrome	2	0	0	0	4%	–
Pigmentation	4	0	–	–	7%	–
Allergy	0	2	–	–	4%	–
Lethargy	13	4	0	0	33%	–
AST/ALT elevation	22	2	0	0	47%	–
Diarrhea	8	2	2	0	23%	4%
Sensory neuropathy	31	9	0	0	78%	–

*Other than sensory neuropathy

Table 4. Incidence of neurotoxicity in FOLFOX regimens

	1–4 Cycles ($n = 9$)			5–8 Cycles ($n = 28$)			9–12 Cycles ($n = 14$)			All cycles ($n = 51$)		
Grade	1	2	3	1	2	3	1	2	3	1	2	3
Sensory neuropathy	5	0	0	19	2	0	7	7	0	31	9	0
	56%	0%	0%	68%	7%	0%	50%	50%	0%	60%	18%	0%

Grade	The oxaliplatin-specific scale (DEB-NTC)			
	0	1	2	3
Dysesthesia and/or paresthesia	No abnormality	Transient dysesthesia and/or paresthesia lasting less than 7 days	Transient dysesthesia and/or paresthesia lasting 7 days or more	Dysesthesia and/or paresthesia with pain or function impairment that interferes with activities of daily living

was reported in 31 patients (61%). Paresthesia lasting 7 days or longer (grade 2) occurred in 9 patients (18%). Peripheral neuropathy appeared in two forms. In the first form, an acute, transient, cold-exacerbated dysesthesia or paresthesia occurred shortly after the administration of oxaliplatin; it affected the hands, feet, perioral area, and throat; and typically lasted for several days after drug administration. In the second form, a delayed-onset, cumulative, dose-related peripheral neuropathy was characterized by paresthesias affecting the hands and feet that did not remit between cycles of treatment. Investigators also reported pharyngolaryngeal dysesthesia in only one patient; however, no patients had a laryngospasm-like syndrome.

Overall, 7 of the 51 patients (14%) required dose modification during treatment; dose reduction was required for oxaliplatin alone in 4 patients, for 5FU alone in 2 patients and for both agents in 1 patient. The majority of dose reductions were by one level (reduction to 65 mg/m^2 oxaliplatin and/or 75% of the starting dose of 5FU). No patients required a second-level dose reduction. The adverse events most commonly leading to dose reduction were neurotoxicity (1 patient in FOLFOX4 and 3 patients in mFOLFOX6) and diarrhea (2 patients in mFOLFOX6). In addition, 2 patients in the mFOLFOX6 setting underwent a dose reduction of oxaliplatin due to allergic reaction. The most common reason for treatment discontinuation was PD.

Antitumor activity

All 51 patients were able to be evaluated for response. Objective responses are listed in Table 5 and Table 6. There was no complete response. The overall objective response rates (in those who underwent first-line or second-line therapy) were 50.0% and 8.7%, respectively (Table 6). Stable disease was achieved in 49% of patients. The tumor control rate (PR + SD) was 80.4%.

Discussion

The recent advent of several new agents for the treatment of metastatic CRC has markedly enhanced the therapeutic armamentarium for this disease. Oxaliplatin in combination with infusional 5FU in the FOLFOX regimens has been shown to be effective in achieving improved response rate, time to progression, and survival time compared with 5FU/LV. In addition, recent large clinical phase III studies (N9741, EFC4584, GERCOR) showed that combination chemotherapy regimens, including irinotecan and oxaliplatin, markedly improved response rates and prolonged median survival over those seen with 5FU/LV),[11-13] and these combination chemotherapy regimens have supplanted 5FU/LV as a standard systemic approach for metastatic CRC. The median survival time (MST) has been gradually pro-

Table 5. Objective responses – (1)

FOLFOX4 (n = 20)				
CR	PR	SD	PD	NE
0	5 (25%) First-line, 3; second-line, 2	12 (60%)	3 (15%)	0
mFOLFOX6 (n = 31)				
0	11 (35.5%) First-line, 11; second-line, 0	13 (41.9%)	7 (22.6%)	0

CR, complete response; PR, partial response; SD, stable disease; PD, progressive disease; NE, not evaluable

Table 6. Objective responses – (2)

First-line (n = 28)				
CR	PR	SD	PD	NE
0	14 (50%) FOLFOX4, 3; mFOLFOX6, 11	11 (39.3%)	3 (10.7%)	0
Second-line (n = 23)				
0	2 (8.7%) FOLFOX4, 2	14 (60.9%)	7 (30.4%)	0

CR, complete response; PR, partial response; SD, stable disease; PD, progressive disease; NE, not evaluable

longed through the use of 5FU/LV with irinotecan and oxaliplatin. Currently, with the addition of molecular targeted agents, an MST of over 20 months has been reported.

Since April 2005, and the approval of oxaliplatin in Japan, clinical practice in this country has been conducted in a major way by extrapolation from the results of clinical trials conducted mainly in large Western phase III studies. The results of the present retrospective study demonstrate the efficacy and feasibility of FOLFOX regimens (FOLFOX4 and mFOLFOX6) as treatment for patients with advanced CRC in the Japanese population, as has been shown in Western populations. In this retrospective analysis study in a Japanese population, neutropenia grade 3/4 occurred in 20% of the patients who were assigned to receive oxaliplatin, but it was nonfebrile, whereas grade 3/4 vomiting and mucositis affected only 4% of the patients, while diarrhea affected 4%.

Lethargy has been described as the most frequent adverse event of the mFOLFOX6 regimen in a recent report by Braun et al.[14] In our study, 17 (33%) patients experienced lethargy similar to general fatigue symptoms.

The cumulative dose-limiting toxicity of oxaliplatin is peripheral sensory neuropathy, which reportedly occurs in about 70%–80% of patients; it typically resolves a few months after discontinuation of treatment, and may be exacerbated by cold stimulation. In our series, paresthesia lasting 7 days or longer was observed in 18% of patients and led to an oxaliplatin dose reduction for four patients after they had received a minimum of seven cycles (or at least 4 months) of chemotherapy.

The mechanism of this neurotoxicity has been elucidated to be as follows: the increased neuronal excitability is due to the action of oxaliplatin on voltage-gated sodium channels through the chelation of calcium by the oxaliplatin metabolite. The prevention of this neurotoxicity is a major goal, taking in to account the wide indications of this drug. Various different approaches have been either previously studied or are now being evaluated, based on pathogenic or practical concepts: (1) modification of the administration schedule; (2) substances acting upon sodium channels, such as calcium-magnesium, carbamazepine, gabapentine, venlafaxine; (3) detoxifying agents and antioxidants, such as glutathione, amifostine, alphalipoic acid, tocopherol; (4) substances used in other kinds of neuropathy, such as glutamine and alphalipoic acid; (5) neurotrophic factors, such as nerve growth factor (NGF), LIF; and (6) oxaliplatin analogs, with a DACH platin, without oxalate. Calcium-magnesium infusion appears to be an efficient and safe approach.

In this study, after September 2005, 32 patients (63%) were administered calcium-magnesium infusion for the prevention of the oxaliplatin-related neurotoxicity. Further studies are necessary for a better understanding and prevention of this potentially severe neurotoxicity.

In terms of antitumor activity, although the response rate (RR) in our population was slightly lower in comparison to that in previous Western clinical studies,[11–13] both of the oxaliplatin-based regimens demonstrated a promising objective RR in the first-line setting (50.0%) and in the tumor control rate (80.4%).

In a GERCOR study, the median survival was 21.5 months in 109 patients allocated to FOLFIRI then FOLFOX6 versus 20.6 months in 111 patients allocated to FOLFOX6 then FOLFIRI (P = 0.99). In first-line therapy, FOLFIRI achieved a 56% RR and 8.5-month median PFS, versus FOLFOX6, which achieved a 54% RR and 8.0-month median PFS (P = 0.26). Second-line FOLFIRI achieved a 4% RR and 2.5-month median PFS, versus

FOLFOX6, which achieved a 15% RR and 4.2-month PFS.[13] Although our study could not evaluate enough data for PFS and MST due to the short observation period after the approval of oxaliplatin in Japan, both the FOLFOX regimens we used seem to be beneficial as first-line and second-line therapy for refractory or advanced CRC in a Japanese population, with an overall response rate which is comparable to Western figures regarding first-line and second-line therapy. FOLFOX6 is the most useful of the FOLFOX regimens because it is simple and can be administered on an outpatient basis. When we use oxaliplatin in FOLFOX regimens, because 85 mg/m^2 is the approved dose for usage in Japan, the treatment is adapted for this dose, even in the mFOLFOX6 regimen.

In conclusion, the FOLFOX regimens we used were found to demonstrate good efficacy as chemotherapy regimens in our population, with an acceptable overall toxicity profile. However, attention must be paid to the occurrence of peripheral sensory neuropathy, which may influence a patient's quality of life, while also limiting the continuation of such treatment.

References

1. Poon MA, O'Connell MJ, Moertel CG, et al. (1989) Biochemical modulation of fluorouracil: evidence of significant improvement of survival and quality of life in patients with advanced colorectal carcinoma. J Clin Oncol 7:1407–1418
2. Levi F, Zidani R, Misset JL (1997) Randomised multicentre trial of chronotherapy with oxaliplatin, fluorouracil, and folinic acid in metastatic colorectal cancer: International Organization for Cancer Chronotherapy. Lancet 350:681–686
3. Giacchetti S, Perpoint B, Zidani R, et al. (2000) Phase III multicenter randomized trial of oxaliplatin added to chronomodulated fluorouracil-leucovorin as first-line treatment of metastatic colorectal cancer. J Clin Oncol 18:136–147
4. Douillard JY, Cunningham D, Roth AD, et al. (2000) Irinotecan combined with fluorouracil compared with fluorouracil alone as first-line treatment for metastatic colorectal cancer: a multicentre randomised trial. Lancet 355:1041–1047
5. Machover D, Diaz-Rubio E, de Gramont A, et al. (1996) Two consecutive phase II studies of oxaliplatin (L-OHP) for treatment of patients with advanced colorectal carcinoma who were resistant to previous treatment with fluoropyrimidines. Ann Oncol 7:95–98
6. Levi F, Perpoint B, Garufi C, et al. (1993) Oxaliplatin activity against metastatic colorectal cancer: a phase II study of 5-day continuous venous infusion at circadian rhythm modulated rate. Eur J Cancer 29A:1280–1284
7. Diaz-Rubio E, Sastre J, Zaniboni A, et al. (1998) Oxaliplatin as single agent in previously untreated colorectal carcinoma patients: a phase II multicentric study. Ann Oncol 9:105–108
8. Becouarn Y, Ychou M, Ducreux M, et al. (1998) A phase II trial of oxaliplatin as first-line chemotherapy in metastatic colorectal cancer patients. J Clin Oncol 8:2739–2744
9. de Gramont A, Vignoud J, Tournigand C, et al. (1997) Oxaliplatin with high-dose leucovorin and 5-fluorouracil 48-hour continuous infusion in pretreated metastatic colorectal cancer. Eur J Cancer 33:214–219
10. Raymond E, Buquet-Fagot C, Djelloul S, et al. (1997) Antitumor activity of oxaliplatin in combination with 5-fluorouracil and the thymidylate synthase inhibitor AG337 in human colon, breast, and ovarian cancers. Anticancer Drugs 8:876–885
11. Goldberg RM, Sargent DJ, Alberts SR, et al. (2004) A randomized controlled trial of fluorouracil plus leucovorin, irinotecan, and oxaliplatin combinations in patients with previously untreated metastatic colorectal cancer. J Clin Oncol 22:23–30
12. de Gramont A, Figer A, Bonetti A, et al. (2000) Leucovorin and fluorouracil with or without oxaliplatin as first-line treatment in advanced colorectal cancer. J Clin Oncol 18:2938–2947
13. Tournigand C, Andre T, de Gramont A, et al. (2004) FOLFIRI followed by FOLFOX6 or the reverse sequence in advanced colorectal cancer: a randomized GERCOR study. J Clin Oncol 22:229–237
14. Braun MS, Adab F, Seymour MT, et al. (2003) Modified de Gramont with oxaliplatin in the first-line treatment of advanced colorectal cancer. Br J Cancer 89:1155–1158

Cancer Chemother Pharmacol (2007) 60:285–293
DOI 10.1007/s00280-006-0382-7

ORIGINAL ARTICLE

Phase I study of TZT-1027, a novel synthetic dolastatin 10 derivative and inhibitor of tubulin polymerization, which was administered to patients with advanced solid tumors on days 1 and 8 in 3-week courses

Kenji Tamura · Kazuhiko Nakagawa · Takayasu Kurata · Taroh Satoh · Toshiji Nogami · Koji Takeda · Shigeki Mitsuoka · Naruo Yoshimura · Shinzoh Kudoh · Shunichi Negoro · Masahiro Fukuoka

Received: 27 July 2006 / Accepted: 30 October 2006 / Published online: 30 November 2006

Abstract
Purpose To determine the maximum tolerated dose (MTD), dose-limiting toxicity (DLT), and pharmacokinetics of TZT-1027 (soblidotin), a dolastatin 10 analogue, in Japanese patients with advanced solid tumors when administered on days 1 and 8 in 3-week courses.
Methods Eligible patients had advanced solid tumors that failed to respond to standard therapy or for which no standard therapy was available, and also met the following criteria: prior chemotherapy ≤2 regimens, Eastern Cooperative Oncology Group (ECOG) performance status ≤1, and acceptable organ function. The MTD was defined as the highest dose at which no more than one of six patients experienced a DLT during course 1. Pharmacokinetic samples were collected in courses 1 and 2.
Results Eighteen patients were enrolled in the present study. Three doses (1.5, 1.65, and 1.8 mg/m^2) were evaluated. Neutropenia was the principal DLT at doses of 1.65 and 1.8 mg/m^2. In addition, one patient also experienced grade 3 pneumonia with neutropenia, and another patient experienced grade 3 constipation, neuropathy, grade 4 neutropenia, and hyponatremia as DLTs at 1.65 mg/m^2. Phlebitis, the most frequent nonhematological toxicity, was improved by administration of additional saline after TZT-1027 administration. The MTD was 1.5 mg/m^2, at which DLT was not observed in a total of nine patients. The pharmacokinetic profile did not differ from that for the European population. One patient with metastatic esophageal cancer achieved partial response, and each of two patients with non-small cell lung cancer had a minor response.
Conclusions When TZT-1027 was administered on days 1 and 8 in 3-week courses to Japanese patients, the MTD was 1.5 mg/m^2 and was lower than the value of 2.4 mg/m^2 in European patients. However, antitumor activity was observed at low doses. TZT-1027 was tolerated well at the MTD, without grade 3 nonhematological toxicities or neutropenia up to grade 2. TZT-1027 is a promising new tubulin polymerization inhibitor that requires further investigation in phase II studies.

Keywords Dolastatin · TZT-1027 · Phase I · Antitubulin · Solid tumors

K. Tamura · K. Nakagawa · T. Kurata · T. Satoh · T. Nogami · M. Fukuoka
Department of Medical Oncology,
Kinki University School of Medicine, Osaka, Japan

K. Takeda · S. Negoro
Department of Clinical Oncology,
Osaka City General Hospital, Osaka, Japan

S. Mitsuoka · N. Yoshimura · S. Kudoh
Department of Respiratory Medicine,
Osaka City University Medical School, Osaka, Japan

K. Tamura (✉)
Department of Medical Oncology,
Kinki University School of Medicine,
Nara Hospital, 1248-1, Otoda, Ikoma,
Nara 630-0293, Japan
e-mail: ktamura@nara.med.kindai.ac.jp

Introduction

TZT-1027 (N^2-(*N*,*N*-dimethyl-L-valyl)-*N*-[(1S,2R)-2-methoxy-4-[(2S)-2-[(1R,2R)-1-methoxy-2-methyl-3-oxo-3-[(2-phenylethyl)amino]propyl]-1-pyrrolidinyl]-1-[(1S)-1-methylpropyl]-4-oxobutyl]-*N*-methyl-L-valinamide) is a

synthesized analogue of dolastatin 10, a compound isolated from the marine mollusk *Dolabella auricularia* [9, 17]. The chemical structures of TZT-1027 and dolastatin 10 are shown in Fig. 1.

In in vitro studies, TZT-1027 exhibited time-dependent cytotoxicity superior to that of other antitumor agents against a variety of murine and human tumor cell lines [19]. TZT-1027 also exhibited antitumor activity against p-glycoprotein (p-gp)-overexpressing and breast cancer resistant protein (BCRP) positive cell lines established from colon cancer H116 and lung cancer PC-6, and was more potent than vincristine, paclitaxel, and docetaxel. The efficacy of TZT-1027 has been attributed to its inhibitory activity on tubulin polymerization. TZT-1027, believed to interact with tubulin in the same domain as the vinca alkaloid-binding region, inhibits the polymerization of microtubule proteins and the binding of GTP to tubulin [12]. In in vivo studies, intravenous injection of TZT-1027 has been shown to potently inhibit the growth of P388 leukemic cells and several solid tumors in mice and to increase life span, with efficacy superior or comparable to that of reference agents, dolastatin 10, cisplatin, vincristine, and 5-fluorouracil [4, 7]. In the xenograft models, furthermore, TZT-1027 reduced intratumoral blood perfusion from 1 to later than 24 h after administration, thus leading to hemorrhagic necrosis of tumor [5, 11, 15]. TZT-1027 exerts antitumor activity through direct cytotoxicity, as well as selective blockade of tumor blood flow, resulting in remarkable antitumor activity. In animal toxicology studies, TZT-1027 had no or little neurotoxic potential in marked contrast to vincristine and paclitaxel which are antimicrotubule agents that have exhibited peripheral neurotoxicity in controlled animal studies [14]. When doses of TZT-1027 were increased, on the other hand, myocardial toxicity was observed in rats and monkeys.

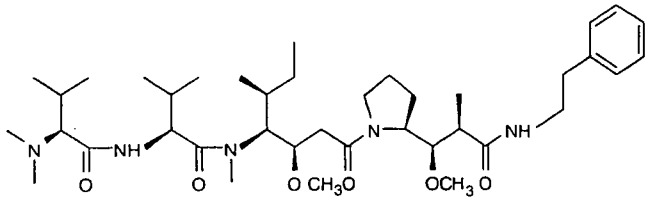

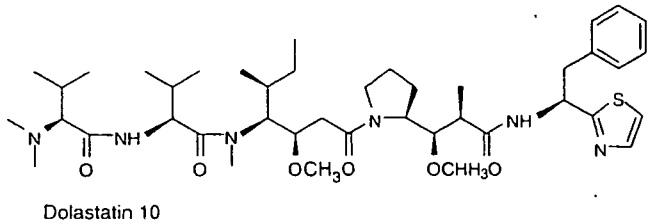

Fig. 1 Structural formulae of TZT-1027 and dolastatin 10

In Japan, a single-dose phase I study was conducted at doses up to 1.35 mg/m^2, but did not reach the MTD. The major toxicity was neutropenia, and nonhematological toxicities included alopecia, malaise, and anorexia. Therefore, a repeated-dose study of TZT-1027 on days 1, 8, and 15 in 4-week courses followed the single-dose study in Japan. Toxicities were similar, with leucopenia and neutropenia as major toxicities. All episodes of grade 4 neutropenia occurred at doses of 1.5 mg/m^2 or higher. Nonhematological toxicities were mild and did not exceed grade 2 in most patients. Neutropenia was observed as a DLT [13, 20], and the recommended dose was 1.8 mg/m^2. In Europe, three phase I studies were conducted. A repeated-dose study of TZT-1027 according to the administration schedule on days 1 and 8 in 3-week courses was performed in the Netherlands. This schedule was chosen based on the previous phase I study in Japan, in which TZT-1027 had been administered on days 1, 8, and 15; however, several patients could not receive TZT-1027 on day 15 due to neutropenia; the dose of TZT-1027 was escalated to 2.7 mg/m^2, with neutropenia and infusion arm pain as DLTs. The recommended dose for phase II studies of TZT-1027 was 2.4 mg/m^2 [2]. Phase II studies are ongoing according to this schedule. Two other administration schedules on day 1 in a 3-week course and on day 1 in a 3- to 4-week course were tested in Germany and Hungary, respectively. In the German study, DLTs—including neutropenia, fatigue, and short-lasting, reversible peripheral neurotoxic syndrome—were observed at 3.0 mg/m^2. On the other hand, the Hungarian study, enrolling exclusively patients with non-small cell lung cancer, was conducted at doses up to 5.6 mg/m^2 [6, 18]. In these studies, the major toxicities were neutropenia, nausea, vomiting, constipation, alopecia, and injection site pain. The pharmacokinetics of TZT-1027 in these studies appeared linear. The rate of TZT-1027 binding to α1-acid glycoprotein, a major plasma protein, was ~95%. In all studies, several patients exhibited a tumor reduction.

Preclinical and clinical data indicated that a suitable administration schedule for the present study would be days 1 and 8 in 3-week courses. The purposes of the present phase I study were to assess the DLTs, to determine the MTD, to observe preliminary antitumor activity, and to study the pharmacokinetics of TZT-1027 that was administered intravenously over 60 min on days 1 and 8 in 3-week courses in Japanese patients with advanced solid tumors. The electrocardiogram (ECG), including QTc interval prolongation, was assessed to estimate cardiovascular side effects.

Patients and methods

Study design

The present study, an open-label, dose-escalating, three-institution phase I study, was conducted in Japanese patients with solid tumors to assess the DLTs, to determine the MTD and preliminary antitumor activity, and to examine pharmacokinetics. A starting dose of 1.8 mg/m^2 was chosen, since this is the recommended dose for the phase II study based on the previous phase I study in Japan, and TZT-1027 was expected to be effective at this dose.

After the MTD was decided, TZT-1027 was administered to three patients at the MTD level to confirm the appropriate recommended dose for phase II studies. TZT-1027 was given intravenously over 60 min with 250 ml of saline on days 1 and 8 in 3-week courses. The present study and the written consent form were approved by the Institutional Review Board. All patients provided informed consent before study entry. The present study was conducted in accordance with the Good Clinical Practice Guidelines as issued by the International Conference on Harmonization and the Declaration of Helsinki.

Patient eligibility

Patients with histologically or cytologically confirmed solid tumors, which were refractory to standard therapy or for which no effective therapy was available, were eligible to participate in the present study. Other inclusion criteria included the following: no prior chemotherapy or radiotherapy within 4 weeks of study entry (within 6 weeks for nitrosoureas, carboplatin, and mitomycin C; and within 2 weeks for local radiotherapy); not more than two previous regimens of chemotherapy; no previous wide-field radiotherapy to >25% of the bone marrow; age 20–74 years; ECOG performance status, 0 or 1; life expectancy, at least 2 months; adequate bone marrow: hemoglobin $\geq$ 8.5 g/dl, absolute neutrophil count (ANC) $\geq$ 1,500/mm^3, platelet count $\geq$ 100,000/mm^3; and normal hepatic functions [serum bilirubin $\leq$ 1.5 mg/dl, and serum aspartate aminotransferase (ALT) and alanine aminotransferase (AST) $\leq$2.5 times the upper limit of normal (ULN), respectively]; and renal function (serum creatinine $\leq$ lower limit of normal). The left ventricular ejection fraction (LVEF), measured by ultrasound cardiography (UCG), had to be $\geq$60%. Patients with symptomatic brain metastases or known extensive bone marrow invasion were excluded.

Treatment and dose escalation

The dose escalation plan consisted of doses of 1.5, 1.65, and 1.8 mg/m^2. At least three patients were evaluated for the MTD at each dose. If one DLT was observed in a cohort, a total of six patients were enrolled at that dose. The dose escalation was discontinued when two or more of six patients experienced a DLT. The MTD was defined as the highest dose at which no more than one of six patients experienced a DLT during course 1.

The DLT was defined as follows: (a) grade 4 neutropenia with fever (>38.0°C) or lasting 5 days or longer; (b) platelet count < 25,000/mm^3; (c) grade 3/4 nonhematological toxicity excluding nausea and vomiting; (d) grade 3/4 nausea and vomiting with intensive support care; (e) inability to receive TZT-1027 on day 8 in course 1, which was defined as ANC < 1,000/mm^3, platelet count < 100,000/mm^3, a DLT by day 8, or the investigator or subinvestigator assessed it to be difficult to initiate administration; and (f) inability to start course 2 up to day 29. Treatment was resumed when meeting all the following criteria: (a) ANC $\geq$ 1,500/mm^3; (b) platelets $\geq$ 100,000/mm^3; (c) total bilirubin $\leq$ 1.5 mg/dl; (d) serum creatinine $\leq$ ULN.

Patients were withdrawn from the present study when they exhibited disease progression or the next course had to be delayed for more than 2 weeks due to any toxicity. The patients were subsequently treated at the dose one level below the level at which the DLT occurred. Toxicity was assessed using the National Cancer Institute Common Toxicity Criteria (version 2.0).

Treatment assessment

Baseline assessment, including a complete medical history, physical examination, vital signs, ECOG performance status, blood counts, serum biochemistry, and urinalysis, was conducted to assess patient eligibility and had to be completed within 7 days before the start of treatment. Routine biochemistry, hematology, and urinalysis were performed weekly during the treatment course and within 72 h prior to its start. ECG, as well as blood pressure and pulse rate monitoring were performed immediately before and at the end of drip infusion on days 1 and 8 and on day 2 in courses 1 and 2, as well as at the end of the study. The QT interval was corrected for heart rate (QTc) with Bazett's formula ($QTc = QT/RR^{0.5}$). LVEF was performed every two courses. Tumor response was evaluated after every course by RECIST.